# MOMENTUM AND ZONAL KINETIC ENERGY CALCULATIONS FOR THE SOUTHERN HEMISPHERE

by

MARVIN ROSENSTEIN

B.S., New York University
(1970)

SUBMITTED IN PARTIAL FULFILLMENT
OF THE REQUIREMENTS FOR THE
DEGREE OF MASTER OF
SCIENCE

at the

MASSACHUSETTS INSTITUTE OF TECHNOLOGY

December, 1972 ( i.e. Feb. 1973)

Signature of Author.....
Department of Meteorology
December 1, 1972

Certified by.....
Thesis Supervisor

Accepted by.....
Chairman, Departmental Committee
on Graduate Students

# MOMENTUM AND ZONAL KINETIC ENERGY CALCULATIONS FOR THE SOUTHERN HEMISPHERE

by

MARVIN ROSENSTEIN

Submitted to the Department of Meteorology on December 1, 1972 in partial fulfillment of the requirements for the degree of Master of Science.

## ABSTRACT

The mean circulations, momentum transports and zonal kinetic energy balance of the Southern Hemisphere are evaluated. The equation used to investigate the energy balance has never been used in previous Southern Hemisphere studies. Momentum transports by vertical eddies are also calculated for the first time. The vertical processes are deduced from observations of the horizontal wind fields by continuity of mass and angular momentum requirements. Results are presented for two data sets. The first is compiled from five years of hemispheric data and represents the most extensive Southern Hemisphere set yet collected. The second is the same as the first but augmented by twenty-six bogus stations. The data for these stations were derived from the work of a previous investigator in an attempt to fill in some of the glaring gaps in the geographical coverage of the original data set. Because significant differences exist between the results of the two data sets, it is concluded that all available data is still insufficient for any reasonably accurate determination of the quantities involved. However, the results do give an indication of some of the more important general circulation processes in the Southern Hemisphere, and in what manner these processes might interact.

Thesis Supervisor: Victor P. Starr
Title: Professor of Meteorology

TABLE OF CONTENTS

LIST OF TABLES

LIST OF FIGURES

# CHAPTER I

## INTRODUCTION

This thesis is a continuation of the research efforts of the Planetary Circulations Project of M.I.T., headed by Prof. V.P. Starr. One of the goals of this project is to better understand the general circulation of the earth's atmosphere through observational studies of the atmospheric balances of angular momentum and kinetic energy of the zonally averaged zonal wind, the latter usually referred to as "zonal kinetic energy" or "ZKE".

The theoretical groundwork for much of the project's efforts was first laid in 1948 by Starr. It had been obvious for some time that symmetrical models of the general circulation which lumped all eddy type action into a parameterized friction term, assumed to be positively viscous, were incorrect and unreal. Picking up on the assertion by Jeffries in 1926 that horizontal eddies of the large scale were significant in the maintainence of the zonal winds, Starr and others proceeded with many observational studies to prove this now well-established fact (see for example Starr and White, 1951). For a compilation of works in this area through 1965, see Starr and Saltzman, 1966.

The phenomenon which Starr dubbed "negative eddy

viscosity" was a revolutionary idea in 1948, but has since been confirmed time and again. This action consists of the transport of angular momentum by horizontal large scale eddies against the gradient of mean angular velocity, thus supplying kinetic energy to the upper level westerlies rather than destroying them. For a complete discussion see Starr, 1968. It has also recently been shown by Starr, Peixoto and Sims (1970), and Rosen (1971), that vertical eddies may often act in this same manner. Unfortunately, this idea has not yet gained as wide a recognition as it should in some meteorological circles due to the acceptance of the much heralded quasi-geostrophic theory (see Phillips , 1963) by many theoreticians.

In recent years, the bulk of the project's efforts has been directed towards the evaluation of the zonal kinetic energy balance of the N. Hemisphere. The data utilized in these studies consist of daily upper wind soundings at 799 stations mainly in the N. Hemisphere, for the 5 year period 5/1/58 - 4/30/63. The objective machine analysis and computational techniques were developed under the direction of J. Welsh while at Travlers Research Center. For discussions of the data library and machine techniques see Starr, Peixoto and Gaut (1970), and Frazier, Sweeton and Welsh (1968).

These investigations have progressed to the point

where the balance has been computed for polar caps of fixed height but increasing latitudinal extent, (Sims, 1969 and 1970), and polar caps of fixed latitudinal extent but increasing vertical depth (Rosen, 1970 and 1971). Also investigated was the effect of missing data upon the computations (Stoldt,1971), and the effect of a land-ocean bias in the geographical distribution of stations (Walker, 1970).

Notable among the more recent studies of the S. Hemisphere are Obasi (1963, 1965), Gilman (1965), Newton (1971) and Newell et. al. (1973). For a history of previous S. Hemisphere studies see Obasi, 1963. Investigation of the S. Hemisphere has lagged behind that of the N. Hemisphere because of the obvious difficulty of lack of data.

It is the purpose of the present study to investigate the balances of angular momentum and zonal kinetic energy in the same manner as has been done for the N. Hemisphere in the project's efforts previously cited. The present investigation differs from those of other S. Hemisphere investigators in several important ways. First, the most extensive set of data, in terms of time period covered, yet compiled for the S. Hemisphere is used. Secondly, a more informative zonal kinetic energy equation is evaluated. This equation is capable of revealing

much more about the physical processes that maintain the zonal circulation than the more simple equations evaluated by previous investigators. Third, for the first time vertical eddy processes are calculated. In previous S. Hemisphere works these processes were for the most part neglected, particularly when deducing the meridional circulation from horizontal eddy transports of momentum.

As previously mentioned, the exact same analysis and computational schemes used in the N. Hemisphere studies are used in the present study. As such, there is nothing truly original in the present work. The significance of this study lies in the vacuum of knowledge concerning the S. Hemisphere. The results that will be presented represent, I feel, the most ambitious attempt yet to fill that vacuum.

# CHAPTER II

## THE ZKE BALANCE EQUATION

### A. Notation.

The notation used is standard. We have a rotating spherical polar co-ordinate system. The following list of symbols and definitions are now presented for future reference by the reader.

$\lambda$ = longitude

$\phi$ = latitude

R = radius

a = constant mean radius of the earth

t = time

P = pressure

$u$ = east-west component of wind

$v$ = north-south component of wind

$w$ = vertical component of wind

$\omega = \frac{dP}{dt}$ = vertical P-velocity

g = constant mean acceleration of gravity

$\overline{(\ )} = \text{time average} = \frac{1}{\Delta t}\int (\ )\, dt$

$(\ )' = \text{temporal deviation} = (\ ) - \overline{(\ )}$

$[(\ )] = \text{zonal average} = \frac{1}{2\pi}\oint (\ )\, d\lambda$

$(\ )^* = \text{spatial deviation} = (\ ) - [(\ )]$

$\tau_F$ = vertical stress due to friction

F = frictional force per unit volume

$\psi$ = mass stream function

$\chi$ = momentum stream function

$\Omega$ = angular velocity of the earth

$V$ = volume

$\vec{V}$ = total velocity vector

$\rho$ = density

B. The equation.

The symmetrical form of the ZKE equation is:

$$\int_V \rho\,[\bar{u}]\,\frac{\overline{\partial u}}{\partial t}\,dV =$$

$$\iint 2\pi\,[\bar{u}]\,[\bar{F}]\,R^2\cos\phi\,d\phi\,dR \qquad \{0\}$$

+ internal horizontal integrals

$$+\iint 2\pi\rho R^2\cos^2\phi\,(\Omega R\cos\phi)\,[\bar{v}]\,\frac{\partial}{R\partial\phi}\left\{\frac{[\bar{u}]}{R\cos\phi}\right\}R\,d\phi\,dR \qquad \{1\}$$

$$+\iint 2\pi\rho R^2\cos^2\phi\,[\bar{u}]\,[\bar{v}]\,\frac{\partial}{R\partial\phi}\left\{\frac{[\bar{u}]}{R\cos\phi}\right\}R\,d\phi\,dR \qquad \{2\}$$

$$+\iint 2\pi\rho R^2\cos^2\phi\,[\bar{u}^*\bar{v}^*]\,\frac{\partial}{R\partial\phi}\left\{\frac{[\bar{u}]}{R\cos\phi}\right\}R\,d\phi\,dR \qquad \{3'\}$$

$$+\iint 2\pi\rho R^2\cos^2\phi\,[\overline{u'v'}]\,\frac{\partial}{R\partial\phi}\left\{\frac{[\bar{u}]}{R\cos\phi}\right\}R\,d\phi\,dR \qquad \{3''\}$$

+ internal vertical integrals

$$+\iint 2\pi\rho R^2\cos^2\phi\,(\Omega R\cos\phi)\,[\bar{w}]\,\frac{\partial}{\partial R}\left\{\frac{[\bar{u}]}{R\cos\phi}\right\}R\,d\phi\,dR \qquad \{4\}$$

$$+\iint 2\pi\rho R^2\cos^2\phi\,[\bar{u}]\,[\bar{w}]\,\frac{\partial}{\partial R}\left\{\frac{[\bar{u}]}{R\cos\phi}\right\}R\,d\phi\,dR \qquad \{5\}$$

$$+\iint 2\pi\rho R^2\cos^2\phi\,[\bar{u}^*\bar{w}^*]\,\frac{\partial}{\partial R}\left\{\frac{[\bar{u}]}{R\cos\phi}\right\}R\,d\phi\,dR \qquad \{6'\}$$

$$+\iint 2\pi\rho R^2\cos^2\phi\,[\overline{u'w'}]\,\frac{\partial}{\partial R}\left\{\frac{[\bar{u}]}{R\cos\phi}\right\}R\,d\phi\,dR \qquad \{6''\}$$

+ vertical boundary integrals at $\phi = \phi_1$

$$+\iint 2\pi\rho R^2\cos^2\phi\,(\Omega R\cos\phi)[\bar{v}]\frac{[\bar{u}]}{R\cos\phi}\,dR \qquad \{7\}$$

$$+\iint 2\pi\rho R^2\cos^2\phi\,[\bar{u}][\bar{v}]\frac{[\bar{u}]}{R\cos\phi}\,dR \qquad \{8\}$$

$$+\iint 2\pi\rho R^2\cos^2\phi\,[\bar{u}^*\bar{v}^*]\frac{[\bar{u}]}{R\cos\phi}\,dR \qquad \{9'\}$$

$$+\iint 2\pi\rho R^2\cos^2\phi\,[\overline{u'v'}]\frac{[\bar{u}]}{R\cos\phi}\,dR \qquad \{9''\}$$

+ horizontal boundary integrals at $R = R_1$

$$-\iint 2\pi\rho R^2\cos^2\phi\,(\Omega R\cos\phi)[\bar{u}]\frac{[\bar{u}]}{R\cos\phi}\,R\,d\phi \qquad \{10\}$$

$$-\iint 2\pi\rho R^2\cos^2\phi\,[\bar{u}][\bar{u}]\frac{[\bar{u}]}{R\cos\phi}\,R\,d\phi \qquad \{11\}$$

$$-\iint 2\pi\rho R^2\cos^2\phi\,[\bar{u}^*\bar{u}^*]\frac{[\bar{u}]}{R\cos\phi}\,R\,d\phi \qquad \{12'\}$$

$$-\iint 2\pi\rho R^2\cos^2\phi\,[\overline{u'u'}]\frac{[\bar{u}]}{R\cos\phi}\,R\,d\phi \qquad \{12''\}$$

For the traditional form of the ZKE equation substitute

$$\{1'\}\ \iint 2\pi\rho R^2\cos^2\phi\,(2\Omega\sin\phi)[\bar{v}]\frac{[\bar{u}]}{R\cos\phi}\,R\,d\phi\,dR \quad \text{FOR } \{1\}$$

AND

$$\{4'\}-\iint 2\pi\rho R^2\cos^2\phi\,(2\Omega\cos\phi)[\bar{u}]\frac{[\bar{u}]}{R\cos\phi}\,R\,d\phi\,dR \quad \text{FOR } \{4\},$$

and delete terms $\{7\}$ and $\{10\}$. The limits of integration are $\int_0^{R_1}\int_{-\pi/2}^{\phi_1}(\quad)\,d\phi\,dR.$

As indicated above the zonal kinetic energy equation can be presented in two forms, the traditional form and

the symmetric form. For a derivation of these equations see Starr and Gaut (1969), Sims (1969) and Rosen (1970). Briefly, the difference between the two forms lies in the formulation of the terms involving $\Omega$, the earth's angular velocity. In the traditional form there are two terms representing the internal generation (or destruction) of ZKE via Coriolis forces acting in the horizontal and the vertical, $\{1'\}$ and $\{4'\}$ respectively. In the symmetrical formulation these two terms are further broken down into two internal integrals and two boundary integrals. The internal integrals $\{1\}$ and $\{4\}$ represent generation due to the transport of earth angular momentum $(\Omega R \cos\phi)$ by mean cell motion against the gradients of angular velocity. The boundary integrals represent transfer of ZKE due to the transport of $(\Omega R \cos\phi)$ by mean cell motion multiplied by the angular velocity at the boundary: $\{7\}$ for the vertical boundary, i.e. latitude wall, and $\{10\}$ for the horizontal boundary, i.e. upper bounding surface. For a complete discussion of these differences see Rosen (1972).

The remaining terms in the equation are as follow. The term $\{0\}$ represents the destruction of ZKE by frictional effects. There are internal generation terms, listed on the left below, due to the transport of relative angular momentum with or against the gradient of mean angular velocity by the six processes listed below; and

there are boundary integrals, listed on the right, due to the transport of relative angular momentum by the same six processes multiplied by the mean angular velocity at the boundary.

| | | |
|---|---|---|
| {2} | mean cell motion in the horizontal | {8} |
| {3'} | transient horizontal eddies | {9'} |
| {3"} | standing horizontal eddies | {9"} |
| {5} | mean cell motion in the vertical | {11} |
| {6'} | transient vertical eddies | {12'} |
| {6"} | standing vertical eddies | {12"} |

Several things were implicitly assumed in writing the equation and should be mentioned. First, as noted by Rosen (1972), the left hand side of the equation satisfies the following identity: $\int \rho[\bar{u}] \frac{\partial \bar{u}}{\partial t} dV =$ $\frac{\partial}{\partial t}\int \rho \frac{[u]^2}{2} dV - \int \rho [u]' \frac{\partial [u]'}{\partial t} dV.$ Since the second term on the right hand side of the identity is most likely negligible when considering a period of five years, we see that the left hand side of our equation is, for all practical purposes, the time averaged time rate of change of the kinetic energy of the zonally averaged zonal flow. Second, storage effects are not considered and are assumed to be negligible. Third, density is assumed constant except in the vertical. Fourth, the upper boundary for the polar caps of greatest vertical depth is taken to be 13 mb in pressure co-ordinates. It is assumed that all stresses at this high level vanish sp that the horizontal boundary integrals are zero here.

Fifth, the lower boundary is assumed to be a smooth

ground fixed at R = 0 or in pressure co-ordinates at P = 1013 mb. It is further assumed that all mean and large scale eddy effects vanish here, $[\tau]$ is zero, and evaporation and precipitation processes are negligible. Thus, there are no boundary integrals at the ground. The assumption of a smooth earth where the pressure is always 1013 mb everywhere may be the major source of error when the equation is evaluated. However, an effort is made to partially correct for this by including a mountain torque term due to the action of pressure differentials in the zonal direction across topographic barriers. We thus include the term $\int_V \frac{[\tau]}{R\cos\phi} \frac{\partial P}{\partial \lambda} dV$. Computation of this term is discussed in a later section.

Lastly, for the sake of completeness, it should be pointed out that boundary terms representing the direct advection of ZKE across boundaries can also be added. If this is done, two more internal integrals must be added which exactly balance the added boundary terms. As noted by Starr and Sims (1970), this makes the equation physically complete. However, these terms are not introduced in the present investigation.

# CHAPTER III

## EVALUATION OF STATISTICS

### A. Method of evaluation of the ZKE equation.

The method of evaluation is the same as that described in Sims (1969), Starr, Peixoto and Sims (1970), and Rosen (1970). The ZKE equation is evaluated in pressure co-ordinates, via the transformation equations: $\frac{\partial p}{\partial R} = -\rho g \Rightarrow \frac{\partial ( )}{\partial R} = -\rho g \frac{\partial ( )}{\partial p}$ and $dr = \left(-\frac{1}{\rho g}\right) dp$, i.e. the familiar hydostatic assumption, and $w = \left(-\frac{1}{\rho g}\right) \omega$ which is not exactly true but accurate enough for our purposes. $\omega$ is the vertical P-velocity and is equal to $\frac{dp}{dt}$. Also we let $R \rightarrow a$, the mean radius of the earth. As most meteorologists know, evaluation in pressure co-ordinates rather than vertical R co-ordinates is much easier due to the constancy of g. The variation of the density $\rho$ in the vertical is no longer a factor. Also, observations are made at constant pressure levels.

The quantity $[\overline{v}]$ is normalized to $[\overline{v}]_m$ due to the inability of instruments to measure $v$ to the degree necessary. Values of $[\overline{v}]$ often are the difference of large numbers of opposite signs. Mass continuity requires that the transport of mass across latitude circles, when integrated in the vertical, be approximately zero. $[\overline{v}]_m$ is therefore obtained by subtracting from $[\overline{v}]$ at each

pressure level the simple vertical mass average of $[\bar{v}]$ at that latitude, i.e. $[\bar{v}]_m = [\bar{v}] - \frac{1}{\Delta P}\int [\bar{v}]\, dP$. In this way continuity of mass is satisfied. It is to be understood that in all statistics to be presented $[\bar{v}]$ is actually $[\bar{v}]_m$ unless otherwise stated.

Conservation of mass also requires that $\overline{\frac{\partial \rho}{\partial t}} + \nabla\cdot[\overline{\rho \vec{v}}] = 0$. Now, noting that $\overline{\frac{\partial \rho}{\partial t}} = 0$, and expanding the divergence term in our spherical co-ordinates, we find that:

$$-\frac{\rho[\bar{v}]}{R}\tan\phi + \frac{\partial(\rho[\bar{v}])}{R\partial\phi} + \frac{2\rho[\bar{w}]}{R} + \frac{\partial(\rho[\bar{w}])}{\partial R} = 0.$$

This equation is satisfied by defining a mass stream function $\psi$ as follows: $\frac{\partial}{\partial\phi}\left(-\frac{\partial\psi}{\partial R}\right) + \frac{\partial}{\partial R}\left(\frac{\partial\psi}{\partial\phi}\right) = 0$ WHERE $2\pi\rho R\cos\phi[\bar{v}] = -\frac{\partial\psi}{\partial R}$ AND $2\pi\rho R\cos\phi[\bar{w}] = \frac{\partial\psi}{R\partial\phi}$.

Changing to P co-ordinates:

$$\frac{2\pi}{g}a\cos\phi[\bar{v}] = \frac{\partial\psi}{\partial P} \text{ AND } \frac{2\pi}{g}a\cos\phi[\bar{\omega}] = -\frac{\partial\psi}{a\partial\phi}.$$

From our knowledge of $[\bar{v}]$ which is retrieved from our data, $\psi$ may be solved for by integrating in the vertical:

$$\psi = \int \frac{2\pi}{g}a\cos\phi[\bar{v}]\, dP.$$

Then $[\bar{\omega}]$ can be solved for via:

$$[\bar{\omega}] = \frac{-g}{2\pi a\cos\phi}\frac{\partial\psi}{a\partial\phi}.$$

The above route must be taken since vertical velocities are not able to be measured but must be inferred.

A similar route is taken to deduce the vertical eddy transport of momentum using conservation of angular momentum. We now have the conservation principle: $\nabla\cdot[\overline{\rho M\vec{v}}] = 0$, where $M = (u + \Omega R\cos\phi)R\cos\phi$. Expanding the

brackets and bar operations and the divergence operator in spherical co-ordinates we find that:

$$-2\sin\phi[\bar{\tau}_{\phi\lambda}]+\cos\phi\frac{\partial}{\partial\phi}[\bar{\tau}_{\phi\lambda}]+3\cos\phi[\bar{\tau}_{R\lambda}]+R\cos\phi\frac{\partial}{\partial R}[\bar{\tau}_{R\lambda}]=0,$$

where

$$\frac{1}{\rho}[\bar{\tau}_{\phi\lambda}]=\Omega R\cos\phi[\bar{w}]+[\bar{u}][\bar{v}]+[\overline{u'v'}]+[\overline{u^*v^*}]$$

and

$$\frac{1}{\rho}[\bar{\tau}_{R\lambda}]=\Omega R\cos\phi[\bar{w}]+[\bar{u}][\bar{w}]+[\overline{uw}']+[\overline{u^*w^*}]+\frac{1}{\rho}[\bar{\tau}_F].$$

It is to be noted in writing the last two equations we have assumed that small scale and molecular scale frictional effects transporting momentum horizontally across vertical surfaces is negligible due to the smallness of horizontal wind shears. However, this is not true for the vertical transports and the term $[\bar{\tau}_F]$ must be included due to significant vertical wind shears. In this manner, the term $\{0\}$ will be absorbed into an internal vertical integral and a horizontal boundary integral involving $[\bar{\tau}_p]$. The conservation of momentum principle can now be expressed as:

$$2\pi R^2\cos^2\phi[\bar{\tau}_{\phi\lambda}]=-\frac{\partial\chi}{\partial R}\quad\text{AND}\quad 2\pi R^2\cos^2\phi[\bar{\tau}_{R\lambda}]=\frac{\partial\chi}{R\partial\phi},$$

where $\chi$ is a momentum stream function. Changing to P co-ordinates we have:

$$\frac{2\pi}{g}a^2\cos^2\phi\{[\bar{u}][\bar{v}]+\Omega a\cos\phi[\bar{v}]+[\overline{u'v'}]+[\overline{u^*v^*}]\}=\frac{\partial\chi}{\partial p},\ \text{AND}$$

$$\frac{2\pi}{g}a^2\cos^2\phi\{[\bar{u}][\bar{\omega}]+\Omega a\cos\phi[\bar{\omega}]+[\overline{u'\omega'}]+[\overline{u^*\omega^*}]+[\bar{\tau}_F]\}=-\frac{\partial\chi}{a\partial\phi}.$$

Since the left hand side of the first equation is capable of direct evaluation from our data, we can solve for $\chi$ by integrating in the vertical starting from some high level where $\chi$ is assumed to be zero, i.e.

$$\chi=\int\frac{2\pi}{g}a^2\cos^2\phi\{\Omega a\cos\phi[\bar{v}]+[\bar{u}][\bar{v}]+[\overline{u'v'}]+[\overline{u^*v^*}]\}dp.$$

From the second equation and our knowledge of $[\bar{\omega}]$ from the conservation of mass principle, the vertical eddies can be solved for: $\{\text{VERT. EDDIES}\} =$

$$\{[\bar{u}'\bar{\omega}'] + [\bar{u}^*\bar{\omega}^*] + [\overline{\tilde{u}\tilde{\omega}}]\} = \frac{-g}{2\pi a^2 \cos^2\phi}\frac{\partial \chi}{a\partial\phi} - \Omega a\cos\phi[\bar{\omega}] - [\bar{u}][\bar{\omega}].$$

Unfortunately, the vertical eddies can not be further separated. We thus combine integrals $\{0\}$, $\{6'\}$, $\{6''\}$ into one integral $\{6's\}$ and integrals $\{0\}$, $\{12'\}$, and $\{12''\}$ into one integral $\{12's\}$. Integrals $\{1'\}$, $\{1\}$, $\{2\}$, $\{3'\}$, $\{3''\}$, $\{7\}$, $\{8\}$, $\{9'\}$, $\{9''\}$ are capable of direct evaluation from our data. Integrals $\{4'\}$, $\{4\}$, $\{5\}$, $\{10\}$, $\{11\}$ are capable of evaluation through our knowledge of $\psi$, and integrals $\{6's\}$ and $\{12's\}$ through our knowledge of $\psi$ and $\chi$. Thus, from just our observations of the $u$ and $v$ wind fields, the entire ZKE equation is capable of evaluation.

The integrands that are presented in the form of meridional cross sections are as follow:

internal horizontal integrands

$$\frac{2\pi}{g} a^2\cos^2\phi\,(\Omega a\cos\phi)[\bar{v}]\frac{\partial}{a\partial\phi}\left\{\frac{[\bar{u}]}{a\cos\phi}\right\} \qquad \{1\}$$

$$\frac{2\pi}{g} a^2\cos^2\phi\,(2\Omega\sin\phi)[\bar{v}]\frac{[\bar{u}]}{a\cos\phi} \qquad \{1'\}$$

$$\frac{2\pi}{g} a^2\cos^2\phi\,[\bar{u}][\bar{v}]\frac{\partial}{a\partial\phi}\left\{\frac{[\bar{u}]}{a\cos\phi}\right\} \qquad \{2\}$$

$$\frac{2\pi}{g} a^2\cos^2\phi\,[\bar{u}^*\bar{v}^*]\frac{\partial}{a\partial\phi}\left\{\frac{[\bar{u}]}{a\cos\phi}\right\} \qquad \{3'\}$$

$$\frac{2\pi}{g} a^2\cos^2\phi\,[\bar{u}'\bar{v}']\frac{\partial}{a\partial\phi}\left\{\frac{[\bar{u}]}{a\cos\phi}\right\} \qquad \{3''\}$$

internal vertical integrands

$$\frac{2\pi}{g} a^2 \cos^2\phi \,(\Omega a \cos\phi)\,[\bar{\omega}]\,\frac{\partial}{\partial P}\left\{\frac{[\bar{u}]}{a\cos\phi}\right\} \qquad \{4\}$$

$$\frac{2\pi}{g} a^2 \cos^2\phi \,(2\Omega\cos\phi)\,[\bar{\omega}]\,\frac{[\bar{u}]}{a\cos\phi}\left(\frac{1}{eg}\right) \qquad \{4'\}$$

$$\frac{2\pi}{g} a^2 \cos^2\phi\,[\bar{u}][\bar{\omega}]\,\frac{\partial}{\partial P}\left\{\frac{[\bar{u}]}{a\cos\phi}\right\} \qquad \{5\}$$

$$\frac{2\pi}{g} a^2 \cos^2\phi\left\{[\overline{u'\omega'}]+[\bar{u}^*\bar{\omega}^*]+[\bar{\tau}_F]\right\}\frac{\partial}{\partial P}\left\{\frac{[\bar{u}]}{a\cos\phi}\right\} \qquad \{6's\}$$

vertical boundary integrands at $\phi = \phi_1$

$$\frac{2\pi}{g} a^2 \cos^2\phi\,(\Omega a\cos\phi)\,[\bar{v}]\,\frac{[\bar{u}]}{a\cos\phi} \qquad \{7\}$$

$$\frac{2\pi}{g} a^2 \cos^2\phi\,[\bar{u}][\bar{v}]\,\frac{[\bar{u}]}{a\cos\phi} \qquad \{8\}$$

$$\frac{2\pi}{g} a^2 \cos^2\phi\,[\bar{u}^*\bar{v}^*]\,\frac{[\bar{u}]}{a\cos\phi} \qquad \{9'\}$$

$$\frac{2\pi}{g} a^2 \cos^2\phi\,[\overline{u'v'}]\,\frac{[\bar{u}]}{a\cos\phi} \qquad \{9''\}$$

horizontal boundary integrands at $P = P_1$

$$\frac{2\pi}{g} a^2 \cos^2\phi\,(\Omega a\cos\phi)\,[\bar{\omega}]\,\frac{[\bar{u}]}{a\cos\phi} \qquad \{10\}$$

$$\frac{2\pi}{g} a^2 \cos^2\phi\,[\bar{u}]\,[\bar{\omega}]\,\frac{[\bar{u}]}{a\cos\phi} \qquad \{11\}$$

$$\frac{2\pi}{g} a^2 \cos^2\phi\left\{[\overline{u'\omega'}]+[\bar{u}^*\bar{\omega}^*]+[\bar{\tau}_F]\right\}\frac{[\bar{u}]}{a\cos\phi} \qquad \{12's\}$$

For the internal integrals $\{1\}$ to $\{6's\}$ the limits of integration are:

$$+\int_{1013}^{P_1}\int_{-\pi/2}^{\phi_1}(\qquad)\,a\,d\phi\,(-dP).$$

The limits are written in this way so that a transport of momentum against the gradient of mean angular velocity

generates ZKE. For example, in $\{3''\}$, if $[\tilde{u}'\tilde{v}']$ is towards the south and we are at around $30^{o}$S, we find that:

$[\tilde{u}'\tilde{v}'] < 0$, $\frac{\partial}{a\partial\phi}\left\{\frac{[\tilde{u}]}{a\cos\phi}\right\} < 0$, $dP < 0$, $(-dP) > 0$, AND $d\phi > 0$.

Thus the integral is positive. Also in $\{6's\}$ we find $\{$vertical eddies$\} < 0$ if the transport of momentum is upwards, $\frac{\partial}{\partial p}\left\{\frac{[\tilde{u}]}{a\cos\phi}\right\} < 0$ if we are at a level below the jet, $(-dp) > 0$ and the integral is again positive. For the vertical boundary integrals the limits of integration are:

$$-\int_{1013}^{p_1} (\qquad)\,(-dP).$$

A transport of momentum towards the south is into the polar cap. Thus, in $\{9''\}$, for example, if $[\tilde{u}'\tilde{v}'] < 0$, $(-dp) > 0$, $\frac{[\tilde{u}]}{a\cos\phi} > 0$, therefore the integral is positive. For the horizontal boundary integrals the limits of integration are:

$$+\int_{-\pi/2}^{\phi_1} (\qquad)\,a\,d\phi.$$

A transport of momentum upwards is out of the polar cap. Thus, in $\{12's\}$, for example, $\{$vertical eddies$\} < 0$, $\frac{[\tilde{u}]}{a\cos\phi} > 0$, $d\phi > 0$ and the integral is negative.

For the traditional term $\{1'\}$ it is to be noted that $\sin\phi < 0$, thus if $[\tilde{v}]$ is northwards, i.e. $> 0$, the integral is negative. If $[\tilde{v}]$ is southward the integral is positive. For the traditional term $\{4'\}$, it is to be noted that this is the only term where the density appears. This expression was inadvertently calculated without the extra $\frac{1}{\rho g}$ term. However, due to the small vertical velocities, $\{4'\}$ is quite small, and the $\frac{1}{\rho g}$ term would not make a significant difference. $\{4'\}$ should be calculated using $\rho$ values of

the standard atmosphere. For completeness sake, since $\cos\phi > 0$, if $[\bar{\omega}]$ is upwards, i.e. negative, the integral of $\{4'\}$ is negative. If $[\bar{\omega}]$ is downwards, the integral is positive.

B. The mountain torque term.

In a previous section, the mountain torque term was introduced. I will now outline how this term is evaluated. In a recent article, Newton (1971) has published values for the mountain torque in $5^{\circ}$ latitude belts for both hemispheres. The term he evaluates is $\tau_x = P_x R \cos\phi$, where $P_x = \sum \int_0^H \frac{\partial p}{\partial \lambda} dR$. $P_x$ is the sum around a latitude circle of the pressure differentials across topographical barriers integrated to the height H of the topographic features. $\tau_x$ is the torque due to $P_x$. We see from the expression $\int \frac{[\bar{u}]}{R\cos\phi} \frac{\partial p}{\partial \lambda} dV$ that the angular velocity should be multiplied point for point with the corresponding $\tau_x$ and then integrated with respect to $\lambda$, $\phi$, and R. Since Newton's torques have already been integrated with respect to the vertical and longitude, we must approximate the true integral by multiplying by an angular velocity $\frac{[\bar{u}]}{a\cos\phi}$ which is representative of that particular latitude band and of the entire vertical column. The winds at 838 mb are taken to be representative of the process. Therefore what is to be done is to compute the average $\frac{[\bar{u}]}{a\cos\phi}$ at 838 mb in each latitude band and multiply by $\tau_x$ in that latitude band.

Table 1. Mountain torque calculations for the Northern Hemisphere.

| Latitude | $\tau_x$ ($10^{25}$erg) | $\frac{[\dot{u}]}{a\cos\phi}$ ($10^{-7}$sec$^{-1}$) | MT ($10^{18}$erg sec$^{-1}$) |
|---|---|---|---|
| 85-90N | -------- | 5.60 | ---------- |
| 80-85 | .03 | 5.60 | .17 |
| 75-80 | .28 | 5.58 | 1.56 |
| 70-75 | .57 | 5.96 | 3.40 |
| 65-70 | .74 | 5.74 | 4.25 |
| 60-65 | .75 | 6.50 | 4.88 |
| 55-60 | -.53 | 8.15 | -4.32 |
| 50-55 | -1.87 | 9.85 | -18.42 |
| 45-50 | -2.04 | 9.95 | -20.30 |
| 40-45 | -1.43 | 8.91 | -12.74 |
| 35-40 | -.06 | 7.46 | -.45 |
| 30-35 | .31 | 4.78 | 1.48 |
| 25-30 | 1.40 | 1.93 | 3.67 |
| 20-25 | 1.69 | -1.79 | -3.03 |
| 15-20 | .70 | -4.54 | -3.18 |
| 10-15 | .43 | -6.04 | -2.60 |
| 5-10 | .88 | -5.61 | -4.94 |
| 0-5 | 1.04 | -4.23 | -4.40 |
| | | | -54.97 |

Table I is the results of this method for the N. Hemisphere based on the wind field computed by Starr, Peixoto and Gaut (1970).

The following is to be noted. When the pressure is higher on the east side of an obstacle, i.e. $\frac{\partial p}{\partial \lambda} > 0$ and $\tau_x > 0$, there is an eastward torque on the atmosphere and the atmosphere is gaining westerly angular momentum. When we have $\frac{\partial p}{\partial \lambda} < 0$ and $\tau_x < 0$, the atmosphere loses westerly momentum. Since $[\bar{u}]^2$ has no dependence on the sign of $[\bar{u}]$, we have the following:

| $\tau_x$ | $\frac{[\bar{u}]}{a\cos\phi}$ | |
|---|---|---|
| + | + | increasing westerly strength = increase ZKE |
| + | - | decreasing easterly strength = decrease ZKE |
| - | + | decreasing westerly strength = decrease ZKE |
| - | - | increasing easterly strength = increase ZKE |

The result for the entire N. Hemisphere volume is $-.55 \times 10^{20}$ erg sec$^{-1}$, i.e. the mountains act to decrease the ZKE. It is interesting to note that the estimate of this effect based on the mountain torque calculation of White (1949) used by our project for the N. Hemisphere ZKE studies is $-.54 \times 10^{20}$ erg sec$^{-1}$, an excellent agreement.

C. Data and machine techniques.

The original data set was compiled from two sources. Stations 1-80 are from a personal data collection of

Dr. J. W. Kidson compiled under the sponsorship of the Atomic Energy Commission while working in the research program of Prof. R. E. Newell at M.I.T. (see Newell et. al., 1973). Stations 81-125 were obtained from the Environmental Data Service of the National Oceanic and Atmospheric Administration at Asheville, No. Carolina.

This data set consists of daily soundings for the five year period 5/1/58 - 4/30/63, with observations of $u$ and $v$ at the pressure levels of 1000, 950, 900, 850, 700, 500, 400, 300, 200, 100, 50 mb. Unfortunately, 20 of these 125 stations were found to have absolutely no data at all pressure levels during this five year span. It was decided to add 20 stations from the IGY 1958 data set of Obasi (1963) in those geographical areas where stations were scarce. This leaves us with a total of 125 stations.

This data set is not homogeneous. Different stations had different lengths of records during various time periods in the five year span. Some stations made daily soundings once a day, some twice a day, and some four times a day. Also, these soundings were not always taken at the same Greenwich time at all stations.

The most serious problems were stations with either no data or very little data at various pressure levels. Only a handful of stations had sufficient data at all pressure levels. For the sake of representativeness it

was decided to establish cut-off criteria. If the number of observations at a particular station at a particular level was less than the cut-off criteria for that pressure level, those observations were omitted.

For the N. Hemisphere ZKE studies the cut-off criteria was 30% of the total possible number of observations in the five year period at each pressure level. If a station did not meet this ctiteria at a particular level it was eliminated at that level. In the present study it was decided to establish different criteria at each pressure level, such that a station was totally eliminated only if the number of observations at every pressure level did not satisfy the criteria at each level. Unfortunately, it was not possible to use criteria anywhere near 30%. Table 2 lists these criteria. The 950 and 900 mb levels were completely discarded due to extreme scarcity of data and the small volume of atmosphere these levels represent.

The % criteria are based on a station making two soundings per day for every day in the five year period. At those stations where four soundings a day were made the % criteria is half the listed value. At those stations which made one sounding a day (the majority), the % criteria is double the listed value. It should be noted that regardless of how many soundings a day were made, or at what times of the day, all observations were weighted

Table 2. Cut-Off criteria for observed data.

| Level mb | % criteria | # observations criteria | # stations satisfying the criteria |
|---|---|---|---|
| 1000 | 2 | 74 | 59 |
| 850 | 4 | 148 | 95 |
| 700 | 5 | 185 | 95 |
| 500 | 4 | 148 | 96 |
| 400 | 4 | 148 | 94 |
| 300 | 3 | 111 | 95 |
| 200 | 2 | 74 | 84 |
| 100 | 3 | 111 | 74 |
| 50 | 2 | 74 | 24 |

equally in the time averaging processes.

The 2% criteria at the 1000 mb and 50 mb levels were deemed the lowest possibly acceptable due to the scarcity of data at these levels. The 850 - 300 mb levels criteria were chosen as was necessary to include 75% of the 125 stations. The criteria at 200 mb was reduced to 2% due to the importance of this jet stream level and 65% of the stations were used here. At 100 mb the criteria was raised to include 60% of the 125 stations. This level was considered less important.

In all, 12 of the 125 stations were totally eliminated due to insufficient data. The 113 stations used are listed in Table 3, and plotted as circles in Figure 1. Of these, 98 are S. Hemisphere stations and 15 are slightly north of the equator. Table 4 shows what levels had no data (marked with an 0) and what levels had insufficient data via the criteria (marked with an x) for each of the stations. It is obvious that each of the pressure levels has a different station distribution.

The calculations were done only for the entire 60 month period. It was felt that there was not enough data to warrant calculations for individual seasons in this S. Hemisphere experiment.

At this point, let us consider several things

Table 3. List of observational stations. Longitude is west from Greenwich.

| Station # | WMO # | Latitude | Longitude | Station Name |
|---|---|---|---|---|
| 1 | 41350 | -.68 | 286.83 | Gan(Maldive Is.) |
| 2 | 43371 | 8.48 | 283.05 | Trivandrum, India |
| 6 | 61900 | -9.72 | 14.42 | Ascension Is. |
| 8 | 61995 | -20.30 | 302.50 | Vacoas (Mauritius) |
| 9 | 63450 | 9.00 | 321.27 | Addis Ababa, Ethiopia |
| 10 | 63741 | -1.30 | 323.25 | Nairobi, Kenya |
| 11 | 63894 | -6.87 | 320.80 | Dar Es Salaam Airport, Tanzania |
| 12 | 64005 | .05 | 341.73 | Mbandaka, Rep. of Congo |
| 13 | 64210 | -4.32 | 344.68 | Kinshasa, " " " |
| 14 | 64360 | -11.60 | 332.47 | Lubumbash, " " " |
| 15 | 64400 | -4.83 | 348.10 | Pointe-Noire, " " |
| 16 | 64501 | -.70 | 351.25 | Port-Gentil, Gabon |
| 18 | 64750 | 9.15 | 341.62 | Ati, Chad |
| 19 | 64870 | 7.28 | 346.68 | Ngaoundere, Cameroon |
| 20 | 64910 | 4.02 | 350.28 | Douala, " |
| 23 | 66160 | -8.85 | 346.77 | Luanda, Angola |
| 24 | 66422 | -15.37 | 347.85 | Mocamedes, " |
| 25 | 67001 | -11.70 | 316.77 | Moroni, Comoro Islands |
| 26 | 67009 | -12.28 | 310.70 | Diego-Suarez, Madagascar |
| 27 | 67085 | -18.90 | 312.47 | Tannanarive, " |
| 28 | 67197 | -25.03 | 313.03 | Port-Dauphin, " |
| 29 | 67241 | -15.02 | 319.33 | Lumbo, Mozambique |
| 30 | 67475 | -10.20 | 328.90 | Kasama, Zambia |
| 32 | 67663 | -14.47 | 331.55 | Broken Hill, " |
| 33 | 67774 | -17.83 | 328.98 | Salisbury, So. Rhodesia |
| 35 | 81405 | 4.83 | 52.37 | Cayenne/Rochambeau, Fr. Guiana |
| 36 | 82400 | -3.83 | 32.42 | Fernando Noronha, Brazil |
| 37 | 82898 | -8.02 | 34.85 | Recife, Brazil |
| 38 | 83781 | -23.55 | 46.63 | Sao Paulo, " |
| 39 | 84129 | -2.17 | 79.87 | Guayaquil, Ecuador |
| 40 | 84631 | -12.10 | 77.02 | Lima, Peru |
| 41 | 91334 | 7.45 | 208.17 | Truk, Caroline Is. |
| 42 | 91348 | 6.97 | 201.78 | Ponape, Ea. Caroline Is. |
| 43 | 91376 | 7.10 | 188.60 | Majuro, Marshall Is. |
| 44 | 91408 | 7.35 | 225.52 | Koror, Palau Is. |
| 45 | 91489 | 2.00 | 157.40 | Christmas Is. |
| 46 | 91517 | -9.42 | 200.03 | Honiara, Br. Soloman Is. |
| 47 | 91643 | -8.52 | 180.80 | Funafuti, Ellice Is. |
| 48 | 91680 | -17.75 | 182.55 | Nandi, Fiji Is. |
| 49 | 91843 | -21.20 | 159.77 | Rarotonga, Cook Is. |
| 50 | 91938 | -17.53 | 149.58 | Tahiti-Faar, Society Is. |
| 51 | 94027 | -6.72 | 213.00 | Lae, New Guinea |

Table 3. Continued.

| Station # | WMO # | Latitude | Longitude | Station Name |
|---|---|---|---|---|
| 52 | 94120 | -12.43 | 229.13 | Darwin Airport, Australia |
| 53 | 94294 | -19.25 | 213.23 | Townsville, " |
| 54 | 94299 | -16.30 | 210.02 | Willis Is., " |
| 55 | 94312 | -20.38 | 241.38 | Port Hedland, " |
| 56 | 94335 | -20.67 | 219.50 | Cloncurry, " |
| 59 | 96996 | -12.08 | 263.12 | Cocos Is. |
| 62 | 61996 | -37.83 | 282.43 | Ile Nouvelle Amsterdam |
| 63 | 67341 | -25.92 | 327.43 | Lourenco Marques, Mozambique |
| 64 | 67633 | -15.27 | 336.90 | Mongu, Zambia |
| 65 | 68032 | -19.98 | 336.58 | Maun, Botswana |
| 66 | 68100 | -22.68 | 345.48 | Swakopmund, So. Africa |
| 67 | 68110 | -22.57 | 342.90 | Windheok, " |
| 68 | 68262 | -25.75 | 331.77 | Pretoria, " |
| 69 | 68406 | -28.57 | 343.47 | Alexander Bay, " |
| 70 | 68588 | -29.97 | 329.05 | Durban, " |
| 71 | 68816 | -33.97 | 341.40 | Capetown, " |
| 73 | 85442 | -23.47 | 70.43 | Antofagasta, Chile |
| 74 | 85543 | -32.78 | 71.53 | Quintero, " |
| 75 | 87157 | -27.47 | 58.98 | M.A. Resistencia, Argentina |
| 76 | 87576 | -34.83 | 58.53 | Ezeiza Aero, " |
| 77 | 91592 | -22.67 | 193.55 | Noumea, New Caledonia |
| 79 | 94300 | -24.88 | 246.35 | Carnarvon, Australia |
| 80 | 94326 | -23.80 | 226.12 | Alice Springs, " |
| 81 | 85801 | -41.47 | 72.93 | Puerto Montt, Chile |
| 82 | 89043 | -77.72 | 41.12 | Elsworth St., Antartic |
| 83 | 91902 | -4.03 | 155.00 | Malden, Line Is. |
| 84 | 91700 | -2.77 | 171.72 | Canton Is. |
| 85 | 91765 | -14.30 | 170.70 | Pago Pago, Samoa |
| 86 | (I)89153 | -79.20 | 147.50 | Little Rockford St., Antartic |
| 87 | (II)89153 | -76.27 | 147.50 | " " " " |
| 89 | 89162 | -78.20 | 162.25 | Little America V, " |
| 90 | 89125 | -80.00 | 120.00 | Byrd Station, " |
| 91 | 68994 | -46.88 | 322.13 | Marion Is., So. Africa |
| 94 | 91530 | -.52 | 193.08 | Nauru Is., Detached Isls. |
| 95 | 89611 | -66.25 | 249.47 | Wilkes, Antartic |
| 96 | 89664 | -77.85 | 193.33 | Mc Murdo, " |
| 97 | 89671 | -72.30 | 189.70 | Hallet, " |
| 98 | 87715 | -38.95 | 68.12 | Neuquen Aero, Argentina |
| 99 | 88890 | -51.70 | 57.87 | Port Stanley |
| 100 | 88952 | -65.25 | 64.27 | Argentine Is., Antartic |
| 102 | 89001 | -70.50 | 2.35 | S.A.N.A.E.Station, " |
| 103 | 89022 | -75.52 | 26.60 | Halley bay, " |
| 104 | 89522 | -70.43 | 335.68 | Baseroi Baudoin, " |

Table 3. Continued.

| Station # | WMO # | Latitude | Longitude | Station Name |
|---|---|---|---|---|
| 106 | 89557 | -78.40 | 272.42 | Soviet Skaya, Antartic |
| 107 | 89571 | -68.55 | 282.07 | Davis, " |
| 108 | 89592 | -66.55 | 267.00 | Mirnyj, " |
| 110 | 89601 | -66.30 | 259.18 | Oazis, " |
| 111 | 89606 | -78.45 | 253.13 | Vostok, " |
| 112 | 89009 | -90.00 | 180.00 | Amundsen-Scott, " |
| 113 | 93060 | -35.90 | 184.88 | Moko Hinau, New Zealand |
| 114 | 93062 | -35.93 | 186.13 | Dar Gaville, " |
| 115 | 93104 | -36.60 | 185.10 | Tiritiri Is., " |
| 125 | 95502 | -66.67 | 219.98 | Dumont Diurville, Antartic |
| 126 | 91958 | -27.62 | 144.33 | Rapa, Austral Islands |
| 127 | 97502 | -.93 | 228.88 | Jefman, Indonesia |
| 129 | 97980 | -8.47 | 219.62 | Merauke/Mopah, " |
| 130 | 94974 | -42.83 | 212.53 | Hobart Airport, Australia |
| 131 | 94610 | -31.93 | 244.05 | Perth Airport, " |
| 132 | 78806 | 8.97 | 79.57 | Howard AFB, Canal Zone |
| 133 | 97690 | -2.50 | 219.52 | Sentani, Indonesia |
| 134 | 85406 | -18.50 | 70.33 | Arica/Chacalluta, Chile |
| 136 | 94510 | -26.42 | 213.72 | Charleville, Australia |
| 137 | 94996 | -29.05 | 192.07 | Norfolk Is., " |
| 138 | 61988 | -19.68 | 296.55 | Rodriguez |
| 139 | 64076 | 1.50 | 329.78 | Bunia, Rep. of Congo |
| 140 | 94374 | -23.38 | 209.52 | Rockhampton, Australia |
| 141 | 87344 | -31.32 | 64.22 | Cordoba Aero, Argentina |
| 142 | 91413 | 9.48 | 221.87 | Yap, Caroline Is. |
| 143 | 94203 | -17.95 | 237.78 | Broome, Australia |
| 144 | 84452 | -6.78 | 79.83 | Chiglayo, Peru |
| 145 | 97560 | -1.16 | 224.00 | Biak/Mokmer, Indonesia |

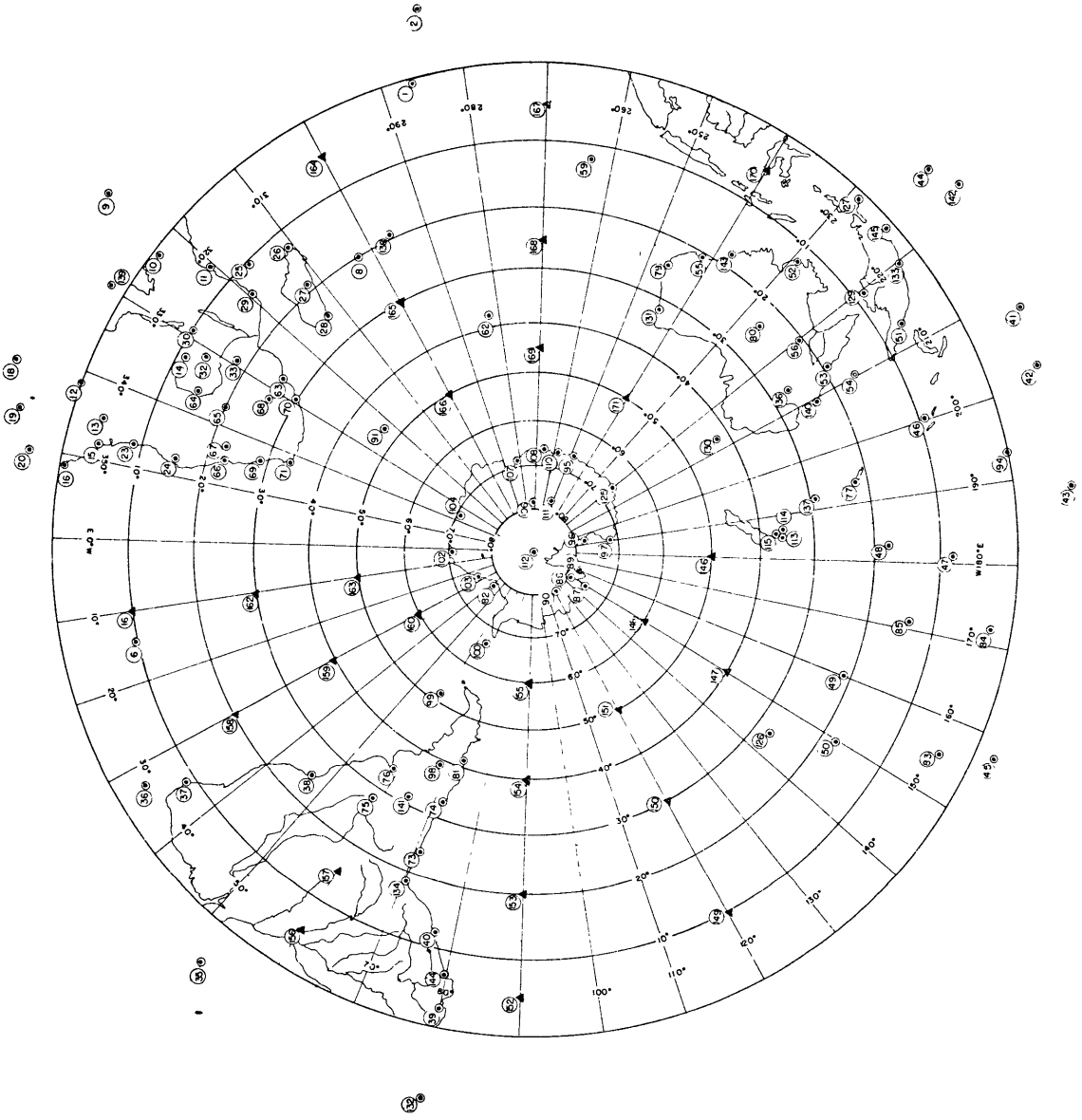

Fig. 1. Geographical distribution of data stations. Circles represent reporting stations, and triangles bogus stations.

Table 4. Pressure levels with no (0) or insufficient (x) reported data for each station.

| Station # | 1000 | 850 | 700 | 500 | 400 | 300 | 200 | 100 | 50 mb |
|---|---|---|---|---|---|---|---|---|---|
| 1 | 0 | | | | | | | | 0 |
| 2 | | | | | | | | | 0 |
| 6 | | | | | | | | | 0 |
| 8 | 0 | | | | | | 0 | 0 | 0 |
| 9 | 0 | 0 | | | | | x | 0 | 0 |
| 10 | 0 | 0 | | | | | | | 0 |
| 11 | 0 | | | | | | | | 0 |
| 12 | x | | | | | | | | 0 |
| 13 | 0 | | | | | | | | 0 |
| 14 | 0 | x | x | x | x | | | | 0 |
| 15 | | | | | | | | | 0 |
| 16 | | | | | | | | | 0 |
| 18 | 0 | | | | | | | | 0 |
| 19 | 0 | | | | | | | | 0 |
| 20 | | | | | | | | | 0 |
| 23 | | | | | | | | | 0 |
| 24 | | x | x | x | 0 | 0 | 0 | 0 | 0 |
| 25 | | x | x | x | x | x | | x | 0 |
| 26 | | | | | | | | | 0 |
| 27 | 0 | | | | | | | | 0 |
| 28 | | | | | | | | | 0 |
| 29 | | | | x | x | 0 | 0 | 0 | 0 |
| 30 | 0 | x | x | x | x | x | | x | 0 |
| 32 | 0 | | | | | | | | 0 |
| 33 | 0 | | | | | | | | 0 |
| 35 | | | | | | | | | 0 |
| 36 | | | | | | | | | 0 |
| 37 | | | | | | | | | 0 |
| 38 | 0 | | | | | | | | 0 |
| 39 | | | | | | | | | 0 |
| 40 | | | | | | | | | 0 |
| 41 | | | | | | | 0 | 0 | 0 |
| 42 | | | | | | | 0 | 0 | 0 |
| 43 | - | | | | | | 0 | 0 | 0 |
| 44 | | | | | | | 0 | 0 | 0 |
| 45 | x | | | | | | | | 0 |
| 46 | | | | | | | | | 0 |
| 47 | 0 | 0 | | | | | | | 0 |
| 48 | 0 | 0 | | | | | | | 0 |
| 49 | 0 | 0 | | | | | | | 0 |
| 50 | | | | | | | | | 0 |
| 51 | | | | | | | | | 0 |
| 52 | | | | | | | | | 0 |
| 53 | | | | | | | | | 0 |

Table 4. Continued.

| Station # | 1000 | 850 | 700 | 500 | 400 | 300 | 200 | 100 | 50 mb |
|---|---|---|---|---|---|---|---|---|---|
| 54 | | | | | | | | | 0 |
| 55 | | | | | | | | | 0 |
| 56 | | | | | | | | | 0 |
| 59 | | | | | | | | | 0 |
| 62 | | | | | | | 0 | 0 | 0 |
| 63 | | | | | | x | x | 0 | 0 |
| 64 | 0 | | | | | | 0 | 0 | 0 |
| 65 | 0 | | | | | | | | 0 |
| 66 | | x | x | x | x | | | x | 0 |
| 67 | 0 | 0 | | | | | | | 0 |
| 68 | 0 | | | | | | | | 0 |
| 69 | | | | | | | 0 | 0 | 0 |
| 70 | | | | | | | 0 | 0 | 0 |
| 71 | | | | | | | 0 | 0 | 0 |
| 73 | | | | | | | | | 0 |
| 74 | | | | | | | 0 | 0 | 0 |
| 75 | | | | | x | 0 | 0 | 0 | 0 |
| 76 | | | | | | x | x | 0 | 0 |
| 77 | x | x | x | x | x | | 0 | 0 | 0 |
| 79 | | | | | | | | | 0 |
| 80 | | | | | | | | | 0 |
| 81 | | | | | | | | | |
| 82 | x | | | | | | | | |
| 83 | | | | | | | | | |
| 84 | | | | | | | | | |
| 85 | | | | | | | | | |
| 86 | 0 | | | | | | | | |
| 87 | 0 | x | x | x | x | x | | x | x |
| 89 | x | | | | | | | | |
| 90 | 0 | 0 | | | | | | | |
| 91 | | | | | | | | | x |
| 94 | | | | | | | | | |
| 95 | | | | | | | | | |
| 96 | | | | | | | | | |
| 97 | | | | | | | | | |
| 98 | 0 | | | | | | | x | x |
| 99 | x | | | | | | | | |
| 100 | x | | | | | | | x | x |
| 102 | x | | | | | | | | |
| 103 | x | | | | | | | | |
| 104 | x | | | | | | | | |
| 106 | 0 | 0 | 0 | | | | x | x | x |
| 107 | 0 | | | | | | | x | 0 |
| 108 | x | | | | | | | | |
| 110 | x | | x | x | x | x | x | x | x |

Table 4. Continued.

| Station # | 1000 | 850 | 700 | 500 | 400 | 300 | 200 | 100 | 50 mb |
|---|---|---|---|---|---|---|---|---|---|
| 111 | 0 | 0 | 0 | | | | | | |
| 112 | 0 | 0 | 0 | | | | | | |
| 113 | 0 | | | | | | | | |
| 114 | 0 | | | | | | | x | x |
| 115 | 0 | | x | | | | | x | x |
| 125 | x | | | | | | | | x |
| 126 | | x | x | x | x | x | x | 0 | 0 |
| 127 | 0 | | x | x | x | x | x | x | x |
| 129 | 0 | | x | x | x | x | x | x | x |
| 130 | x | | | | | | | | |
| 131 | x | | | | | | | | |
| 132 | | | | | | | | | |
| 133 | 0 | | x | x | x | x | x | x | x |
| 134 | | | | | x | x | 0 | 0 | 0 |
| 136 | 0 | | | | | | | | x |
| 137 | | | | | | | | | x |
| 138 | | | | x | x | x | x | 0 | 0 |
| 139 | 0 | | | x | x | x | x | 0 | 0 |
| 140 | 0 | | | | | | | x | x |
| 141 | | | | | | | | | x |
| 142 | | | | | | | | | |
| 143 | | | | | | | | | x |
| 144 | | | x | x | x | x | 0 | 0 | 0 |
| 145 | 0 | | x | x | x | x | x | x | 0 |

concerning the computer technique of analysis. The computer does horizontal analyses of the wind field statistics at each of the 9 pressure levels listed in Table 2. The machine begins its analysis with an initial guess field chosen so as to reduce the number of iterations necessary to analyze the station data. These initial fields provide a shape for the final analyzed wind fields but do not carry much weight when considering magnitudes. They also insure continuity in the vertical since the initial guess field at each level (except 1000 mb) is the analyzed field at the level below. At 1000 mb the initial guess field is taken from what we shall call Crutcher's Data Set (see Van Loon et. al., 1971) made available by Dr. A. H. Oort of the Geophysical Fluid Dynamics Laboratory at Princeton, New Jersey. The final analyzed values are printed out on a polar stereographic grid.

From the analyzed maps at the 9 standard pressure levels, values of the wind statistics at 50 mb intervals from 988 to 38 mb and at $2^{\circ}$ latitude intervals from 11N to 89S are obtained by linear interpolation between the standard levels with respect to height, and by linear interpolation between the horizontal grid points with respect to latitude. Zonal averages around each latitude value are done at each of the 20 pressure levels to produce meridional cross sections. The integrations in the Rosen method of polar caps of increasing depth are for 1013 mb

to 963 mb , 1013 mb to 913 mb, etc., up to 1013 mb to 13 mb. The integration in the Sims method for polar caps of increasing latitudinal extent are for 90S to 88S, 90S to 86S, etc., up to 90S to 0S. The reason for picking odd values of latitude and the 38 - 988 mb levels of pressure in the cross section is now apparent. The values represent the midpoints of the volumes used in the integrations.

One last point concerning machine technique. At 1000 mb, after the computer has analyzed the $\bar{u}$ and $\bar{v}$ fields for the polar stereographic grid, points that normally have a surface pressure much less than 1000 mb, i.e. are much above sea level, are set to the value zero. All these zero values are then figured into the zonal averaging process. What should be done is to simply omit these grid points. However, this is an enormous programming problem. The only other alternative is to leave these "underground" grid points with their analyzed non-zero values. The choice is a difficult one, but it was decided during the N. Hemisphere ZKE studies that it is physically less incorrect to set them to zero. The only region where this may have a great effect in the S. Hemisphere is in the Antartic which attains heights close to 700 mb in the 70S to 90S range. Therefore, the cross section analyses in the Antartic at low levels should not be taken too seriously and is in fact fictitious. It is doubtful that this has much of an effect on the integrations considering the small volume of atmosphere

affected.

As seen in Figure 1, there are great gaps in the geographical distribution of stations, particularly over the oceans. It was felt that the machine analysis of the horizontal wind fields would be too greatly smoothed due to these data scarce regions, with the result of unreasonably weak winds. It was therefore decided to make two sets of calculations. One is for the data set already described which is called data set I. The other is for this set augmented with 26 bogus stations chosen in order to fill in the spatial gaps in coverage. The augmented data set is called data set II. Table 5 is a list of the bogus stations. They are plotted in Figure 1 as triangles. The $\overline{u}$ and $\overline{v}$ values for the levels from 850 to 50 are from Obasi, 1963. They are simple averages of summer (Apr. - Sept.) and winter (Oct.- March) values picked off Obasi's horizontal $\overline{u}$ and $\overline{v}$ maps for these periods in 1958. The values of $\overline{u}$ and $\overline{v}$ at 1000 mb are from Crutcher's data set.

By creating additional winds, it was also necessary to include the requisite horizontal transports of momentum to physically maintain these winds. If this were not done the strengthened winds would draw on a false supply of eddy transport of momentum in the vertical. Values of $\overline{u'v'}$ for the 850-50 levels were picked off Obasi's maps. There was

Table 5. List of bogus stations derived from the work of Obasi (1963).

| Station # | Station Name | Latitude | Longitude * |
|---|---|---|---|
| 146 | MR1 | 50S | 180W |
| 147 | MR2 | 40 | 150 |
| 148 | MR3 | 60 | 150 |
| 149 | MR4 | 10 | 120 |
| 150 | MR5 | 30 | 120 |
| 151 | MR6 | 50 | 120 |
| 152 | MR7 | 5 | 90 |
| 153 | MR8 | 20 | 90 |
| 154 | MR9 | 40 | 90 |
| 155 | MR10 | 60 | 90 |
| 156 | MR11 | 5 | 60 |
| 157 | MR12 | 15 | 60 |
| 158 | MR13 | 20 | 30 |
| 159 | MR14 | 40 | 30 |
| 160 | MR15 | 60 | 30 |
| 161 | MR16 | 10 | 0 |
| 162 | MR17 | 30 | 0 |
| 163 | MR18 | 50 | 0 |
| 164 | MR19 | 5 | 300 |
| 165 | MR20 | 30 | 300 |
| 166 | MR21 | 50 | 300 |
| 167 | MR22 | 5 | 270 |
| 168 | MR23 | 25 | 270 |
| 169 | MR24 | 45 | 270 |
| 170 | MR25 | 5 | 240 |
| 171 | MR26 | 50 | 240 |

* West from Greenwich.

no way to obtain suitable values of $\overline{u'v'}$ at 1000 mb or of $\overline{u^*v^*}$ at any levels. However, it is felt that the omission of these is not serious as they are generally quite small.

# CHAPTER IV

## PRESENTATION OF RESULTS

In this chapter the results in the form of meridional cross sections, latitudinal profiles and tables of three groups of statistics (wind, momentum and zonal kinetic energy) are presented with comments upon the main features of these results. In the next chapter these will be briefly discussed with regards to previous Northern and Southern Hemispheric studies.

### A. Wind Statistics.

Figure 2 contains the meridional cross sections of $[\bar{u}]$ and $\frac{[\bar{u}]}{a\cos\phi}$, and Figure 3 of $[\bar{v}]$, $[\bar{v}]_m$ and $\psi$.

The basic features of $[\bar{u}]$ are pretty much the same for both data sets except for the magnitudes involved. Positive values indicate westerlies. The zonal winds of set I are weaker than those of set II. The former shows a double jet center of 20.7 m sec$^{-1}$ at 43S and 20.3 at 37S; the latter has a jet of 26.0 m sec$^{-1}$ at 44S. The zonal winds continue to be stronger for set II throughout the depth of the atmosphere, with a value near the surface of 5.8 m sec$^{-1}$ at 49S compared to .3 for set I. The changeover from easterlies to westerlies at the surface in low latitudes occurs at 28S for set II and 34S for set I. Thus, set II not only has stronger westerlies, but these also cover a larger

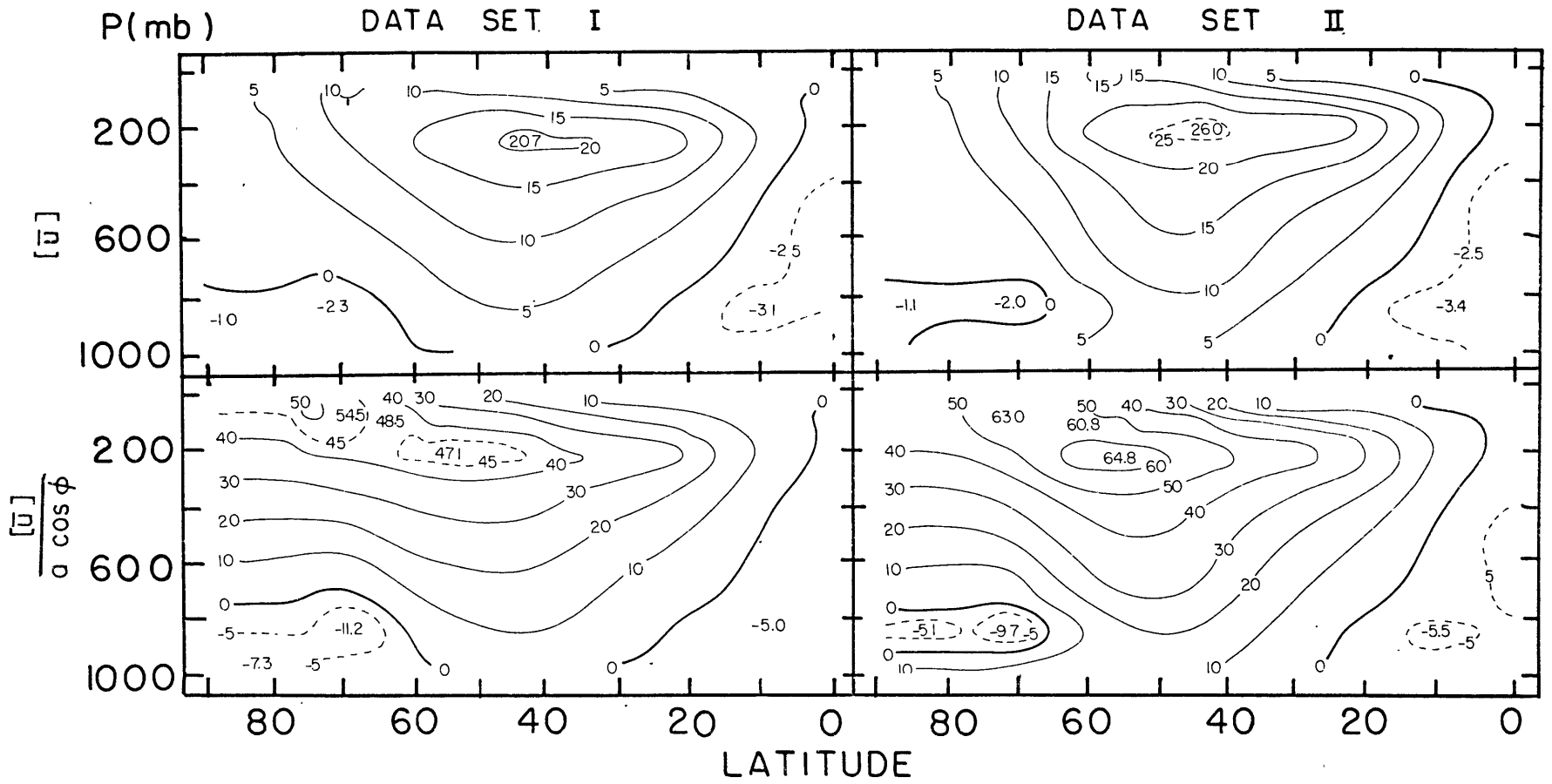


Fig. 2. Meridional cross sections of the mean zonal wind (in units of m $sec^{-1}$) and angular velocity (in units of $10^{-7}$ $sec^{-1}$).

latitudinal extent. One other significant difference is at low levels in the polar region where westerlies persist for set II. As discussed previously, the analysis in this area is not to be trusted due to the height of the Antartic continent.

In the cross sections for the angular velocity $\frac{[\bar{u}]}{a\cos\phi}$, positive values are again westerlies. These maps have in general the same characteristics as those for $[\bar{u}]$. The jet centers are shifted towards the pole and tend to break up into several closed maxima at high latitudes in the 50-100 mb range. Obviously, this must be due to the variation of the cos $\phi$ factor.

In the cross sections of $[\bar{v}]$ positive values indicate southerlies (towards the north). The magnitudes on these maps do not mean very much physically due to the difficulty of accurately measuring and calculating this quantity. But note the preponderance of southerlies, particularly for set II. This is physically impossible due to mass continuity as previously discussed. On this basis, it would appear that set I may be more reliable.

More sense can be made out of the $[\bar{v}]_m$ maps. Again, positive values are southerlies. These two maps are quite similar now with regards to distribution of northerlies and southerlies, except in mid-latitudes where set II has the high level southerlies extending further towards the

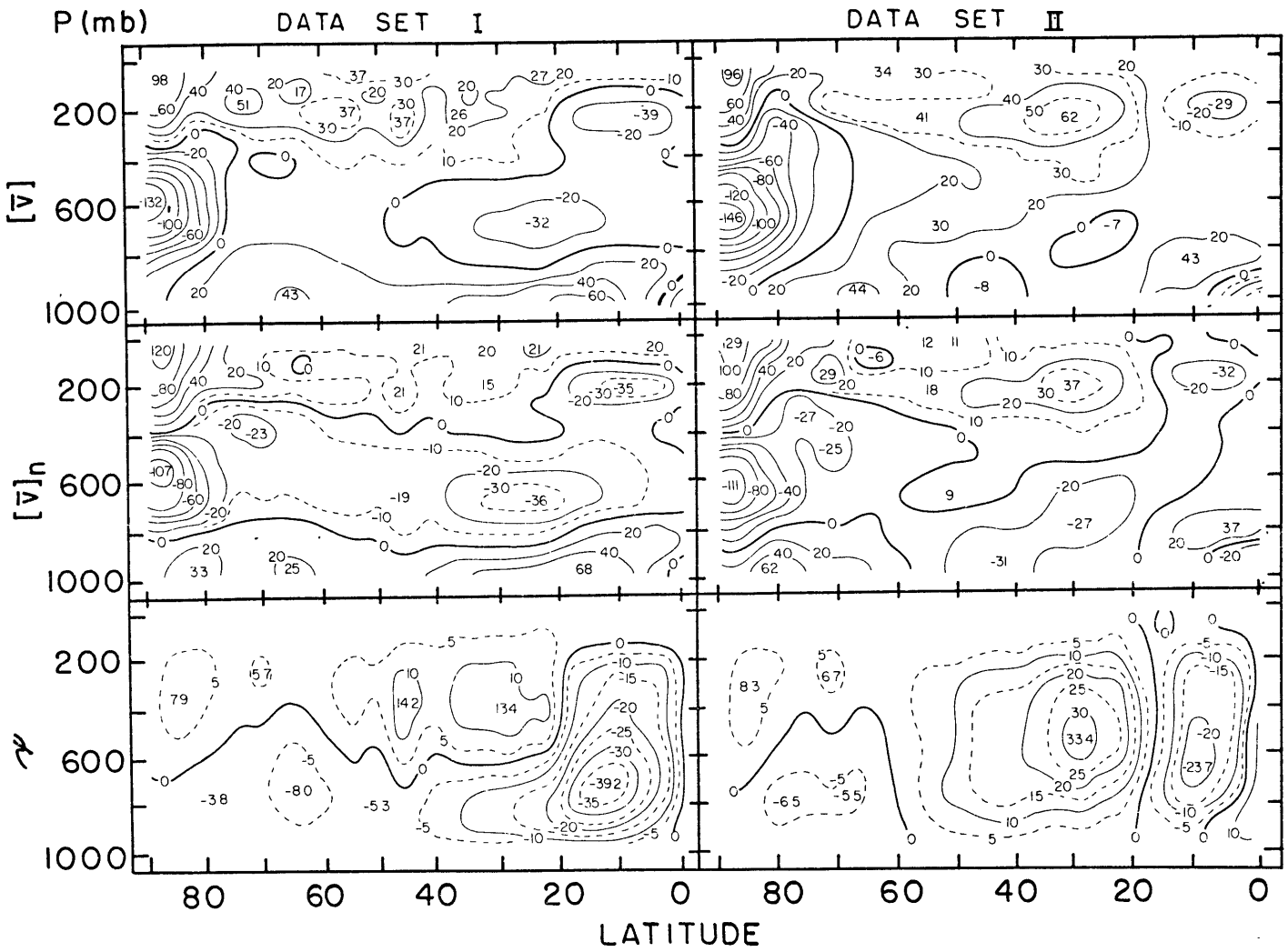


Fig. 3. Meridional cross sections of the mean uncorrected North-South wind, corrected North-South wind (both in units of cm $sec^{-1}$), and mass stream function (in units of $10^{12}$ gm $sec^{-1}$)

ground than set I, and the belt of low level southerlies that appears for set I disappears. Set II implies a very large indirect cell in mid-latitudes with a smaller direct cell in low latitudes. In polar regions an indirect cell at high levels and a direct one at low levels is indicated. Set I points to an indirect cell above a direct one over most of the 0-90S range except at low latitudes where a more pronounced Hadley Cell is implied.

The cross sections for the mass stream function confirm the above remarks. On these maps positive values indicate an indirect cell. For set II we do find a large and strong indirect cell from 20S to 60S, with a center of $33.4 \times 10^{12}$ gm $sec^{-1}$ at 29S, and a smaller, weaker Hadley Cell at low latitudes with a center of $-23.7 \times 10^{12}$ at 11S. In the polar regions of 60-90S there is a weak indirect cell at high levels and a weak direct cell at low levels. Set I shows a larger and stronger Hadley Cell with a center of $-39.2 \times 10^{12}$ gm $sec^{-1}$ at 13S. This cell slopes downwards towards high latitudes extending all the way to the pole. At higher levels we do find a weak indirect cell from about 20S to the pole. It is strongest and of deepest vertical extent from about 25S to 50S, with centers of $14.2 \times 10^{12}$ at 47S and $13.4 \times 10^{12}$ at 29S.

It should be pointed out that the very large values of $[\bar{v}]_m$ above the pole are not inconsistent with the small

values of $\psi$ in this region because the length of the latitude circles here are very small. This argument can be seen from the equation $\psi = \int \frac{2\pi}{g} a \cos\phi [\bar{v}]_m dp$, where cos $\phi$ is quite small near the pole.

Figure 4 contains latitudinal profiles of the vertical averages $(\frac{1}{\Delta p}\int (\ ) dp\ )$ of $[\bar{u}]$, $\frac{[\bar{u}]}{\cos\phi}$ and $[\bar{v}]$.

On the $[\bar{u}]$ profile positive values indicate westerlies. The two profiles are quite similar. Set I has a maximum of 10.8 m sec$^{-1}$ at 43S, while set II has a larger maximum of 15.4 at 47S. Both data sets have the changeover from easterlies to westerlies at 11S. Not much need be said about the profiles of $\frac{[\bar{u}]}{\cos\phi} = a \times$ angular velocity. Set I has a maximum of 16.0 m sec$^{-1}$ at 51S; set II has a maximum of 24.6 at 55S.

The profiles of $[\bar{v}]$ are quite important. As previously discussed, these are profiles of the corrections subtracted from $[\bar{v}]$ to obtain $[\bar{v}]_m$. As such, they are a good measure of the reliability of the two data sets. It is seen that set I appears to be better from this standpoint, as mentioned in our discussion of the cross sections of $[\bar{v}]$. Set I has a magnitude of about 20 cm sec$^{-1}$ from 55S to 75S, while set II is about 20-25 cm sec$^{-1}$ from 25S to 75S.

B. Momentum statistics.

Figure 5 contains the meridional cross sections of

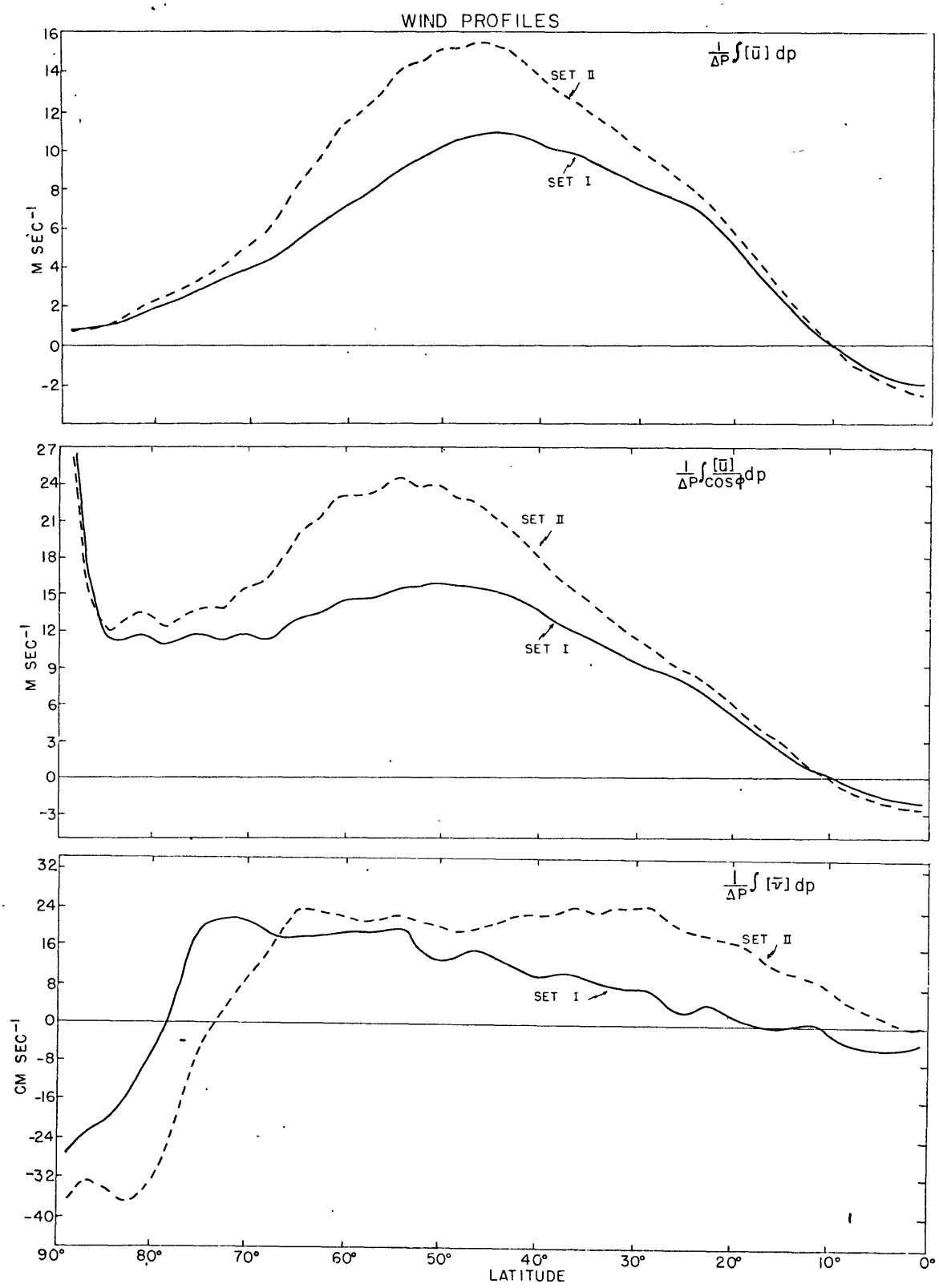


Fig. 4. Latitudinal profiles of the mean zonal wind, angular velocity multiplied by the earth's mean radius, and north-south wind.

$a^2\cos^2\phi\,[\bar{u}'\bar{v}']$ and $a^2\cos^2\phi\,[\bar{u}^*\bar{v}^*]$, and Figure 6 of $a^2\cos^2\phi\,[\bar{u}][\bar{v}]_m$ and $a^2\cos^2\phi\,\{[\bar{u}'\bar{v}'] + [\bar{u}^*\bar{v}^*] + [\bar{\tau}_R]\}$.

The cross sections of $a^2\cos^2\phi\,[\bar{u}'\bar{v}']$ (= transport of relative angular momentum by horizontal transient eddies) are similar in pattern. Negative values indicate a polewards transport. For both data sets there is very strong polewards transport at the jet stream level in low to mid-latitudes, with maxima of $-63.6\times10^{21}$ cm$^4$ sec$^{-2}$ at 23S and $-91.9\times10^{21}$ at 25S for sets I and II respectively. These values are consistent with the stronger zonal jet of set II being slightly poleward of the weaker jet of set I. For both data sets the transient eddies transport momentum horizontally into the jet against the gradient of angular velocity. This is negative viscosity. At higher latitudes the transport changes to equatorwards in both data sets, again against the gradient of angular velocity and into the jet stream.

The cross sections of $a^2\cos^2\phi\,[\bar{u}^*\bar{v}^*]$ (= transport of relative angular momentum by horizontal standing eddies) are not quite as similar as the transient eddy transport maps are. Data set I has much more transport by standing eddies than set II. This agrees with our picture of a stronger and more regular zonal circulation in set II. Set I has equatorwards maxima of $18.5\times10^{21}$ cm$^4$ sec$^{-2}$ at 23S and $14.4\times10^{21}$ at 1S, both at the jet stream level. This

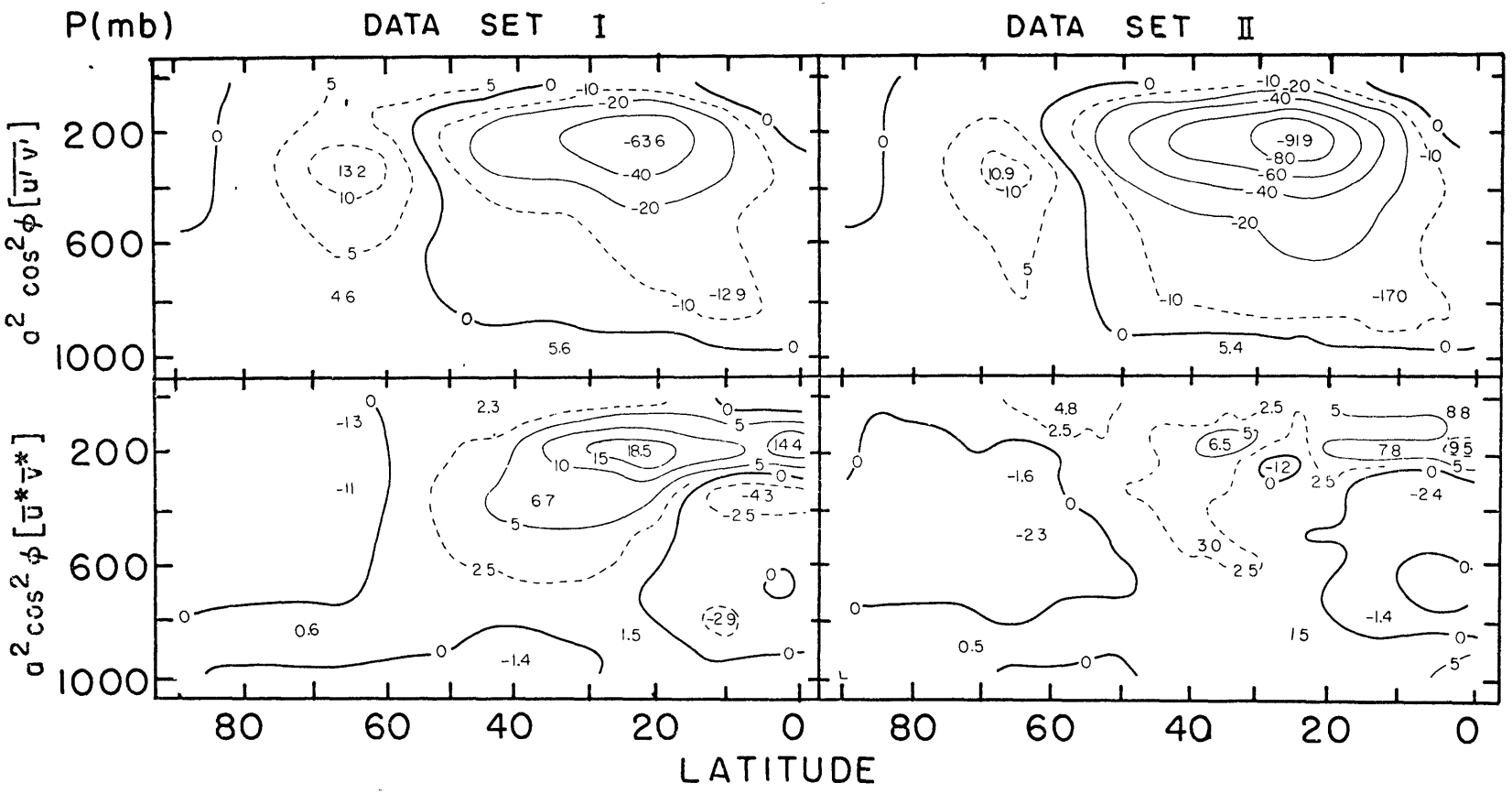


Fig. 5. Meridional cross sections of the mean horizontal transport of relative momentum by transient eddies and standing eddies in units of $10^{21}$ cm$^4$ sec$^{-2}$.

is roughly 1/3 the magnitude of the transient eddy transport maximum. The corresponding values for set II are $6.5 \times 10^{21}$ at 35S and $9.5 \times 10^{21}$ at 1S, roughly 1/10 the transient eddy transport maximum. Here the standing eddies of both data sets act to subtract momentum horizontally from the westerly jet stream. For both data sets as well, there is weak polewards transport throughout most of the depth of the atmosphere at high latitudes, again acting to subtract momemtum from the jet. There is also a region of polewards transport at low latitudes from roughly 900 to 300 mb. But this transport is generally much weaker than the equatorwards transport above.

The cross sections of $a^2 \cos^2\phi [\bar{u}][\bar{v}]_m$ (= transport of relative angular momentum by mean horizontal cell motion) also reflect the stronger zonal and meridional circulations of data set II in mid-latitudes. This set has strong equatorwards transport throughout mid-latitudes with a large maximum at the jet stream level of $43.6 \times 10^{21}$ cm$^4$ sec$^{-2}$ at 29S, about 1/2 that of the transient eddy transport maximum. There is very weak polewards transport at high latitude mid-levels. These two transports both act to subtract momentum from the jet. There is also somewhat stronger polewards transport at low latitudes. For data set I the equatorwards maximum at the jet stream level is substantially less than that of setII, with a value of $13.7 \times 10^{21}$ at 47 S, roughly 1/4 the transient eddy transport

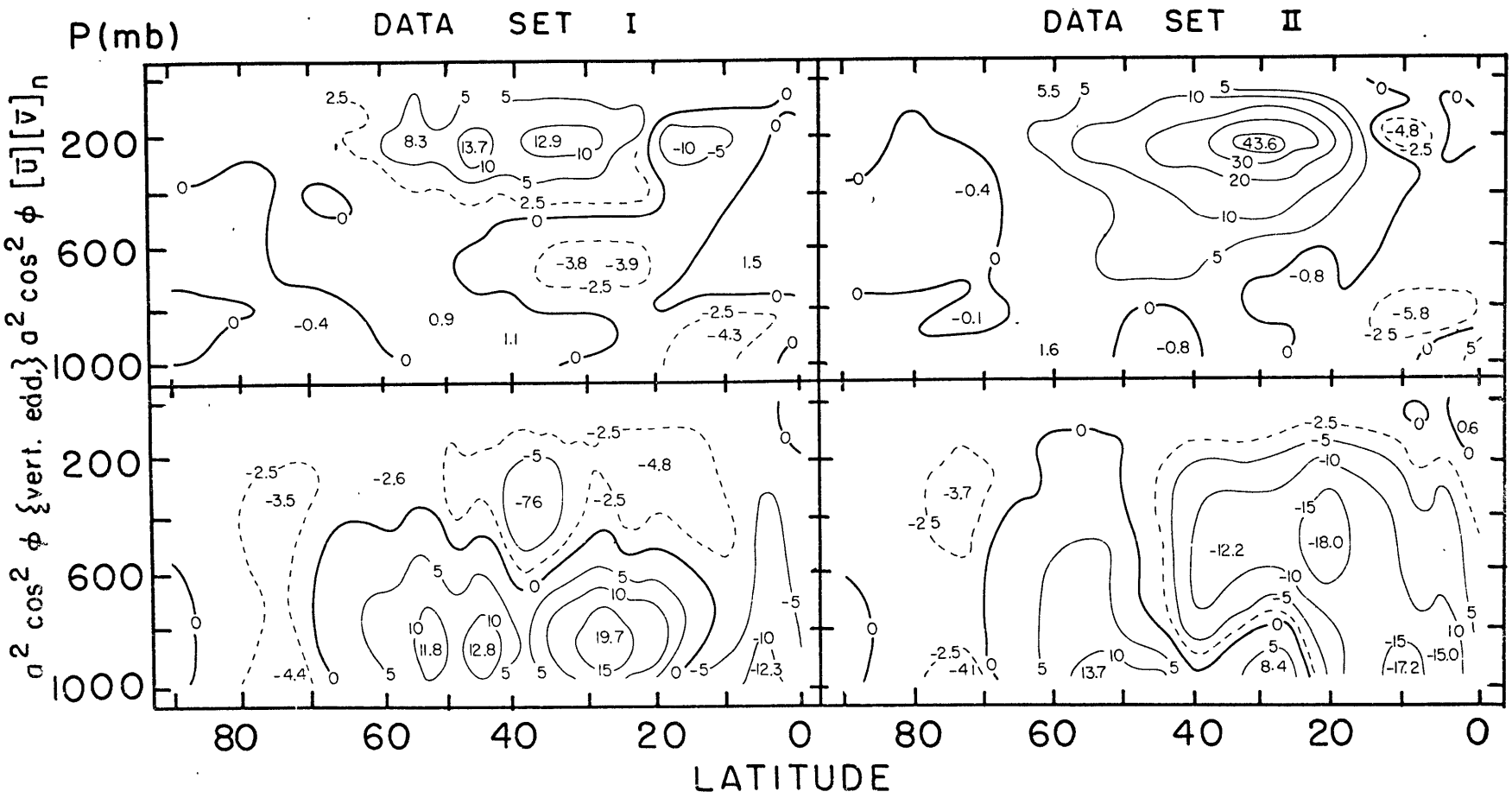


Fig. 6. Meridional cross sections of the mean transport of relative momentum by horizontal cell motion ( in units of $10^{21}$ cm$^4$ sec$^{-2}$ ) and vertical eddies of all types and scales ( in units of $10^{19}$ erg sec$^{-2}$).

maximum. There are now distinct centers of polewards transport beneath the equatorwards maximum and at low latitude high levels. The latter is due to the stronger Hadley Cell of data set I.

A summary of the above three mechanisms in the region of 25 to 35S, north of the jet, is as follows:

| | Data Set I | | Data Set II | |
|---|---|---|---|---|
| | maximum | direction | maximum | direction |
| Transient eddies | -64 | polewards | -92 | polewards |
| Standing eddies | +19 | equatorwards | +7 | equatorwards |
| Mean cell motion | +13 | equatorwards | +44 | equatorwards |

Thus, in both data sets, the standing eddies and mean cell motion act to subtract momentum horizontally from the jet. The former is more important for set I, and the latter for set II. However, in both sets the transport by horizontal transient eddies against the gradient of the jet dominates.

Lastly, in the cross sections of $a^2\cos^2\phi\{\text{VERT. EDDIES}\}$ (= transport of relative angular momentum by vertical eddies of all types and scales) positive values indicate downwards transports. For both data sets there are upwards transports at all levels in high and low latitudes, with maxima near the surface. Data set I has downwards transports in the lower half of the atmosphere from about

15 to 70S with an absolute maximum of $19.7 \times 10^{19}$ erg $sec^{-2}$ at 27S, and upwards transports into the jet in the upper half of the atmosphere with a maximum just below the jet stream level of $-7.6 \times 10^{19}$ at 39S. The vertical eddies of set II transport much more momentum upwards in order to help maintain the stronger jet of this set. The primary maximum is $-18.0 \times 10^{19}$ at 21S. The downwards maximum near the surface is less than that for set I with a value of $13.7 \times 10^{19}$ at 53S. The region of downwards transport between 50 and 70S extends to higher levels than in set I. However, the downwards transport between 15 and 50S in set I has been greatly reduced in magnitude, vertical extent and latitudinal extent in set II.

In general, the above results for the vertical eddies fit in very well with our previous thoughts about the angular momentum balance of the atmosphere. The concept of negative viscosity in the vertical appears to be confirmed. Also, where there are surface easterlies indicating the atmosphere is gaining angular momentum via surface friction, we find upwrds transports in the surface layers. Conversely, in the regions of surface westerlies we find downwards transports near the surface.

Figure 7 contains latitudinal profiles of the vertical averages of the same four quantities as in Figures 5 and 6, but divided by $a^2$.

For the horizontal transient eddies, we see for set I net polewards transport from 0 to 53S, with a maximum of $-5.54$ m$^2$ sec$^{-2}$ at 23S, and net equatorwards transport from 53S to the pole, with a maximum of 1.69 at 65S. For set II we have the same pattern: polewards transport from 0 to 57S, with a larger maximum of $-8.73$ at 25S, and equatorwards transport from 57S to the pole, with a maximum of 1.47 at 67S. The vertically integrated zonal jet is at 43S and 47S for sets I and II respectively. These positions correspond to roughly the midpoints of the regions of convergence of transport of momentum by horizontal transient eddies, 23S to 65S for set I and 25S to 67S for set II. Note that since the jet in set II is slightly south of the jet in set I, so is the region of convergence. The stronger jet of set II also requires more convergence of momentum into it than that for set I. This convergence is reflected by the slopes of the latitudinal profiles of the horizontal transports. The slope of the horizontal transient eddy term is indeed greater for set II than for set I.

On the profiles of the transports by horizontal standing eddies, we find for both data sets equatorwards transport from 60S to the equator, and very small polewards transport from 60S to the pole. Maxima are 1.17 m$^2$ sec$^{-2}$ at 29 S and .58 at 35S for sets I and II respectively. The jets of both data sets are now in regions of divergence

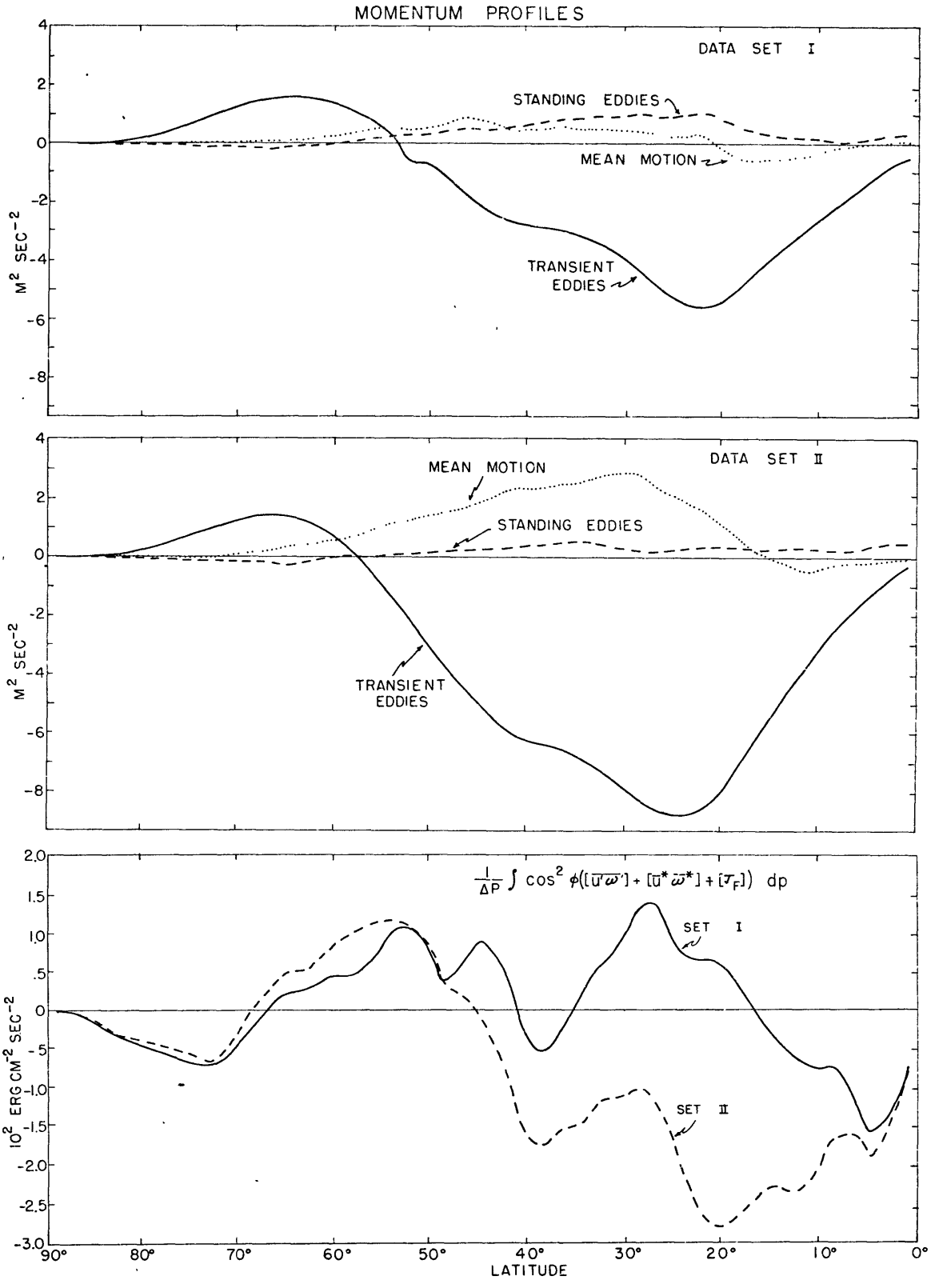


Fig. 7. Latitudinal profiles of the mean transport of relative momentum by horizontal transient eddies, standing eddies and cell motion, and by vertical eddies of all types and scales.

of momentum. As expected from the cross sections for this term, the effect is greater for set I.

For the mean cell motion transport, there is equatorwards transport from 90S to 22S with a maximum of .92 $m^2 sec^{-2}$ at 47S, polewards transport from 22S to 5S, and very weak equatorwards transport from 5S to 0S, all for set I. For set II there is a much stronger region of equatorwards transport from about 75S to 15S with a maximum of 2.89 at 29S caused by the strong and large indirect cell of this data set. Note that the jet is again in a divergence region, particularly for set II.

Below is a summary of the three mechanisms discussed above:

| | Data Set I | | Data Set II | |
|---|---|---|---|---|
| | maximum | jet in region of | maximum | jet in region of |
| Transient eddies | -5.5 | convergence | -8.7 | convergence |
| Standing eddies | +1.2 | divergence | +.6 | divergence |
| Mean cell motion | +.9 | divergence | +2.9 | divergence |

The relative importance of these mechanisms and the manner in which they act so as to support or work against the jet stream is in excellent agreement with the summary previously presented of the mechanisms at the jet stream level only. Which only proves that action at the jet stream level dominates over action at the other levels.

Finally, the profiles for the vertical eddy transport of momentum are quite dissimilar. For set I there is upwards transport from 0 to 17S, 36 to 41S, and 67S to the pole. Maximum value is $-1.54 \times 10^{2}$ erg cm$^{-2}$ sec$^{-2}$ at 5S. There is net downwards transport from 17 to 36S and 41 to 67S. Maximum is $1.40 \times 10^{2}$ at 27S. The agreement with the cross section for the vertical eddies is obvious in low and high latitudes. In middle latitudes, evidently, the downward transports in the lower half of the atmosphere dominate over the upward transports in the upper half except for the 36 to 41S region. For set II, there is upwards transport from 0 to 46S and 69S to the pole, with a larger maximum of $-2.76 \times 10^{2}$ at 21S. From 46S to 69S there is net downwards transport with a smaller maximum of $1.17 \times 10^{2}$ at 55S.

C. ZKE statistics.

1. Internal horizontal processes.

Figure 8 contains the meridional cross sections of integrands $\{1'\}$, $\{1\}$ and $\{2\}$, and Figure 9 of $\{3'\}$ and $\{3''\}$.

For the cross sections of $\{1'\}$, the integrand evaluated is $\frac{2\pi}{g} a^2 \cos^2\phi \, (2\Omega \sin\phi) [\overline{v}]_m \frac{[\overline{u}]}{a\cos\phi}$. This term represents the generation of mean zonal kinetic energy by Coriolis forces acting in the horizontal. It is

contained in the traditional form of the ZKE equation only and is normally one of the major terms in the ZKE balance.

For both data sets, we find the largest and dominating magnitudes at the jet stream level in mid-latitudes. Maxima are $-12.4 \times 10^{6}$ cm sec$^{-1}$ at 47S and $-23.3 \times 10^{6}$ at 33S for sets I and II respectively. These negative generations are due to the upper level southerlies of the indirect cells being turned westward by the Coriolis force, thus decreasing the strength of the upper level westerlies. Since set II has the stronger indirect cell, this effect is much more pronounced for this set.

For the cross sections of $\{1\}$, the integrand evaluated is $\frac{2\pi}{g} a^2 \cos^2\phi \, (\Omega a \cos\phi) [\bar{v}]_m \frac{\partial}{a \partial \phi} \left\{ \frac{[\bar{u}]}{a \cos\phi} \right\}$. This term represents the generation of mean zonal kinetic energy by the transport of earth momentum $(\Omega a \cos\phi)$ with or against the horizontal gradient of angular velocity by the mean horizontal cell motion. It is contained in the symmetric form of the ZKE equation only and is normally one of the major terms in the ZKE balance.

On both cross sections there are large centers of positive generation at low latitude high levels due to the upper level northerlies of the Hadley Cells transporting $\Omega$-momentum polewards against the gradient of angular velocity. These positive generation regions slope downwards towards mid-latitude lower levels due to the

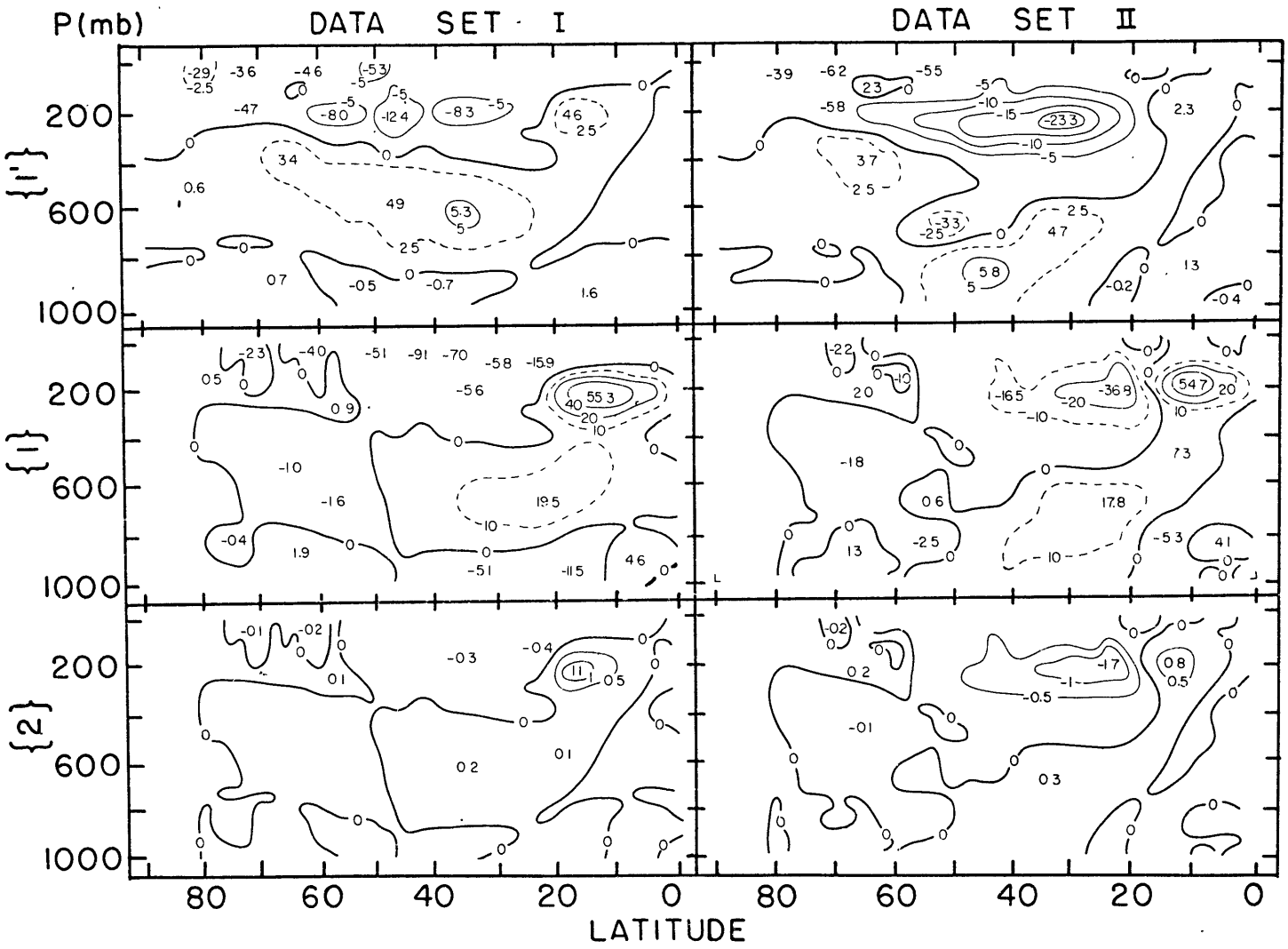


Fig. 8. Meridional cross sections of the internal horizontal integrands $\{1'\}$, $\{1\}$ and $\{2\}$ in units of $10^6$ cm$^2$ sec$^{-1}$.

low level northerlies of the indirect cell of set II and the northerlies between the low level direct and upper level direct cells of set I. Maxima are $55.3 \times 10^6$ cm $sec^{-1}$ at 13S and $54.7 \times 10^6$ at 11S for sets I and II respectively. In mid-latitude upper levels there is negative generation on both cross sections because of the upper level southerlies of the indirect cells. The maxima here are less than those for the positive generation areas to the north because the cos $\phi$ factor tends to place emphasis on lower latitudes. However, the maximum for set II, $-36.8 \times 10^6$ at 23S, is much larger than that for set I, $-15.9 \times 10^6$ at 23S, reflecting the stronger indirect cell of set II.

For the cross sections of $\{2\}$, the integrand evaluated is $\frac{2\pi}{g} a^2 \cos^2\phi \, [\bar{u}][\bar{v}] \frac{\partial}{a\partial\phi}\left\{\frac{[\bar{u}]}{a\cos\phi}\right\}$. This term represents the generation of mean zonal kinetic energy by the transport of relative momentum with or against the horizontal gradient of angular velocity by the mean horizontal cell motion. It is contained in both formulations of the ZKE equation and is not normally one of the major terms in the ZKE balance for either equation.

Once again the stronger Hadley Cell of set I and the stronger Ferrel Cell of set II are reflected. Largest magnitudes are at the jet stream level in low latitudes for set I due to the upper level northerlies of the Hadley Cell. Maximum is $1.1 \times 10^6$ cm $sec^{-1}$ at 16S. For set II, the

upper level southerlies of the Ferrel Cell produce a maximum of $-1.7 \times 10^{6}$ at 23S.

The reason for the much smaller magnitude of term $\{2\}$ as compared to term $\{1\}$ is apparent. In place of the factor $(\Omega a \cos\phi)$ we have the term $[\bar{u}]$, which is about two orders of magnitude smaller. Also, since the inherent uncertainties in $[\bar{v}]_m$ are multiplied by a much larger number in term $\{1\}$ than in term $\{2\}$, the evaluations of the former are more uncertain. However, it is felt that the basic features discussed above are physically valid and fairly computationally sound. Lastly, the apparent similarity of pattern for terms $\{1\}$, $\{1'\}$ and $\{2\}$ is probably due to the dependence upon $[\bar{v}]_m$ in all three terms.

For the cross sections of $\{3'\}$, the integrand evaluated is $\frac{2\pi}{g} a^2 \cos^2\phi \, [\bar{u}^* \bar{v}^*] \frac{\partial}{a \partial \phi} \left\{ \frac{[\bar{u}]}{a \cos\phi} \right\}$. This term represents the generation of mean zonal kinetic energy by the transport of relative momentum with or against the horizontal gradient of angular velocity by horizontal standing eddies. It is contained in both formulations of the ZKE equation and is not normally one of the major terms in the ZKE balance for either equation.

For both data sets, weak negative generation prevails due to transports down the gradient of angular velocity, particularly equatorwards transports north of the mean jet at low latitude high levels. Maxima are

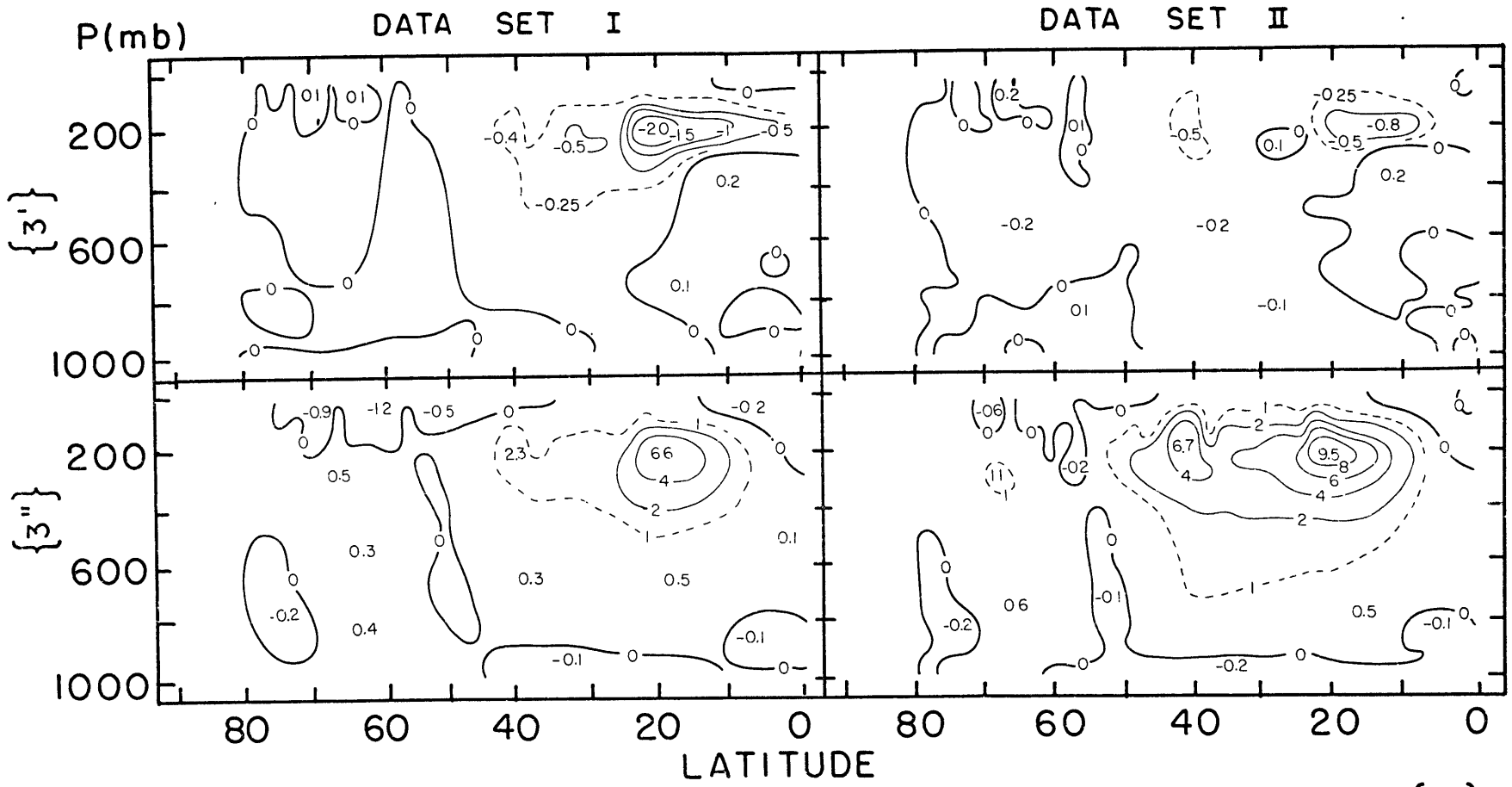


Fig. 9. Meridional cross sections of the internal horizontal integrands $\{3'\}$ and $\{3''\}$ in units of $10^6$ cm$^2$ sec.$^{-1}$

$-2.0\times10^{6}$ cm$^2$ sec$^{-1}$ at 21S and $-.8\times10^{6}$ at 13S for sets I and II respectively. The larger negative generation of set I corresponds to the greater horizontal standing eddy transport of that set, as previously discussed.

For the cross sections of $\{3''\}$, the integrand evaluated is $\frac{2\pi}{g} a^2 \cos^2\phi \, [\bar{u}'\bar{v}'] \frac{\partial}{a\partial\phi}\left\{\frac{[u]}{a\cos\phi}\right\}$. This term represents the generation of mean zonal kinetic energy by the transport of relative momentum with or against the horizontal gradient of angular velocity by horizontal transient eddies. It is contained in both formulations of the ZKE equation and is normally one of the major terms in the ZKE balance for either equation.

As expected from the cross sections of the transient eddy transports in Figure 5, positive generation prevails due to equatorwards transports south of the jet and polewards transports north of the jet, both counter-gradient. The generation is, of course, larger for data set II. Maxima are $6.6\times10^{6}$ cm$^2$ sec$^{-1}$ and $9.5\times10^{6}$, both at 21S, for sets I and II respectively.

2. Internal vertical processes.

Figure 10 contains the meridional cross sections of integrands $\{4'\}$ and $\{4\}$, and Figure 11 of $\{5\}$ and $\{6's\}$.

For the cross sections of $\{4'\}$, the integrand

evaluated is $\frac{2\pi}{g} a^2 \cos^2\phi\,(2\Omega\cos\phi)[\bar{\omega}]\frac{[\bar{u}]}{a\cos\phi}$.
This term represents the generation of mean zonal kinetic energy by Coriolis forces acting in the vertical. It is contained in the traditional form of the ZKE equation only and is not normally a major term in the ZKE balance. As noted previously, the correct form for this term is the one above multiplied by $(\frac{1}{\rho g})$. However, the above term is so small that omitting the $(\frac{1}{\rho g})$ factor does not make a significant difference.

The cross sections serve only to delineate positive generation areas from negative ones. This is why the assumption above is justified. The cross sections show rather erratic behavior. This is because $[\bar{\omega}]$ is related to $[\bar{v}]_m$ through continuity requirements and is subject to even more uncertainties than $[\bar{v}]_m$. This term owes its smallness to that of $[\bar{\omega}]$. The other terms that depend directly upon $[\bar{\omega}]$ ( $\{4\}$ and $\{5\}$ ) are larger because the multiplying factors are much larger.

For the cross sections of $\{4\}$, the integrand evaluated is $\frac{2\pi}{g} a^2 \cos^2\phi\,(\Omega a\cos\phi)[\bar{\omega}]\frac{\partial}{\partial p}\left\{\frac{[\bar{u}]}{a\cos\phi}\right\}$.
This term represents the generation of mean zonal kinetic energy by the transport of $\Omega$-momentum with or against the vertical gradient of angular velocity by the mean vertical cell motion. It is contained in the symmetric form of the ZKE equation only and is normally one of the

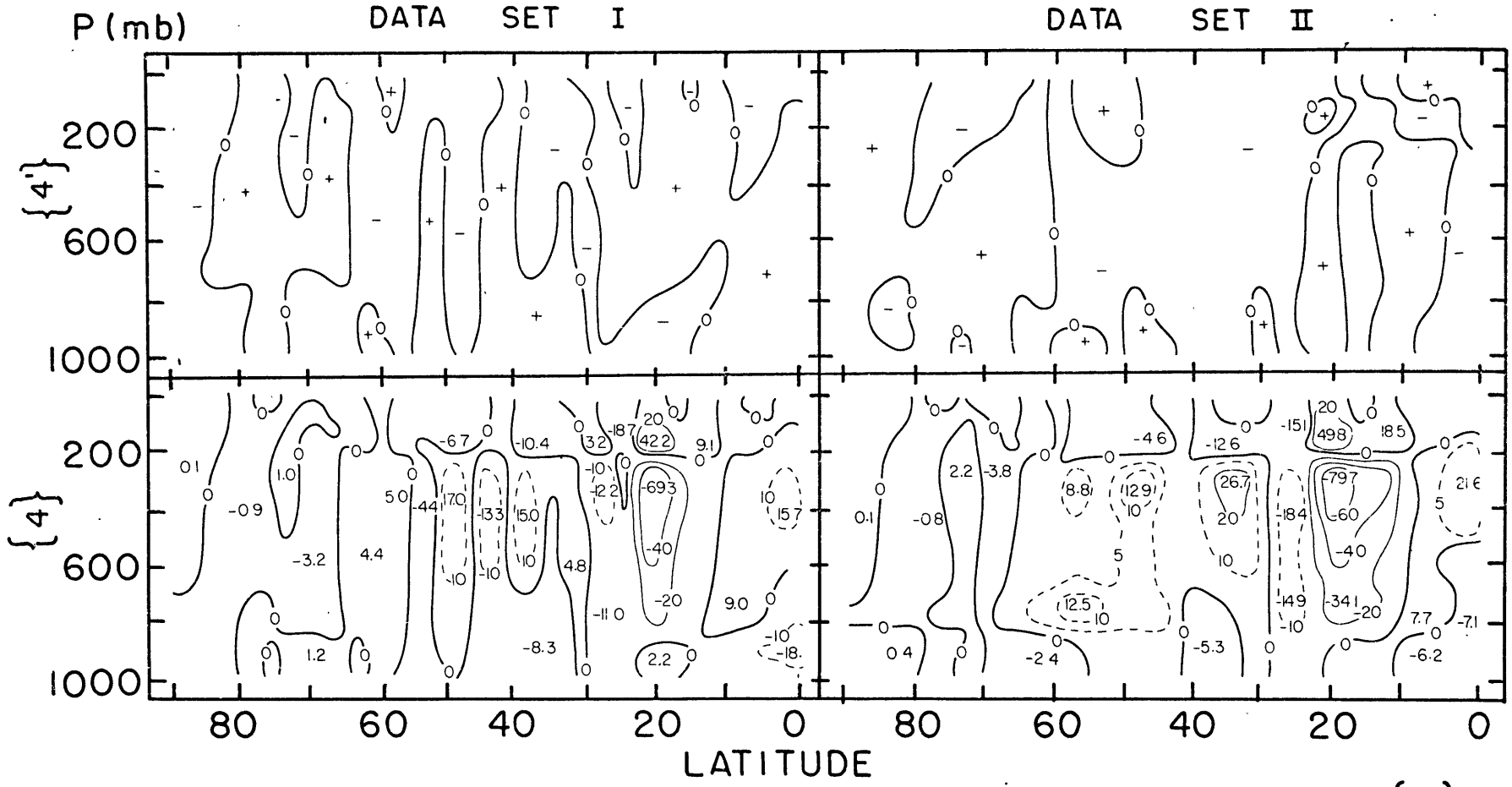


Fig. 10. Meridional cross sections of the internal vertical integrands $\{4'\}$ and $\{4\}$ in units of $10^6$ cm$^2$ sec$^{-1}$.

major terms in the ZKE balance.

The cross sections for both data sets show erratic behavior of extreme values, which is again due to the uncertainties in $[\bar{w}]$ being multiplied by the very large term $(\Omega a \cos\phi)$. However, as was stated for term $\{1\}$, it is felt that the basic features to be discussed are physically valid. As was also true for $\{1\}$, the $\Omega$ term places emphasis on lower latitudes. For both sets, there are centers of positive generation at very low latitudes below the jet level associated with the rising branch of the Hadley Cell transporting $\Omega$-momentum upwards and countergradient. There are larger centers of negative generation below the jet due to the descending branches of the Hadley and Ferrel Cells. Maxima are $-69.3 \times 10^6$ cm $^2$ sec $^{-1}$ and $-79.7 \times 10^6$, both at 21S, for sets I and II respectively. In middle latitudes below the jet level, upward motion in the indirect cells producing positive generations dominates for the most part, especially for set II. In low and middle latitudes the sign of the generation reverses at the jet stream level due to the reversal of the vertical gradient of angular velocity. Most striking examples of this are at 21S where we go from a maximum of $-69.3 \times 10^6$ below the jet to $+42.2 \times 10^6$ above the jet in set I, and $-79.7 \times 10^6$ to +49.8 in set II. For the most part, generations (both positive and negative) are larger for set II than for set I because of the stronger overall

circulations of the former.

For the cross sections of $\{5\}$, the integrand evaluated is $\frac{2\pi}{g} a^2 \cos^2\phi [\bar{u}][\bar{\omega}] \frac{\partial}{\partial P}\left\{\frac{[\bar{u}]}{a\cos\phi}\right\}$. This term represents the generation of mean zonal kinetic energy by the transport of relative momentum with or against the vertical gradient of angular velocity by the mean vertical cell motion. It is contained in both formulations of the ZKE equation and is not normally a major term in the ZKE balance for either equation.

These cross sections have magnitudes much smaller than those for $\{4\}$ due to the size difference between $(\Omega a\cos\phi)$ and $[\bar{u}]$, as previously discussed for terms $\{1\}$ and $\{2\}$. Both data sets show the largest negative generations are associated with the descending branches of the Ferrel and Hadley Cells just below the jet level. Maxima are $-2.1\times10^{6}$ cm $\sec^{-1}$ and $-2.8\times10^{6}$, both at 21S, for sets I and II respectively. As was true for $\{4\}$, set II has stronger generations than set I, particularly in mid-latitudes below the jet where set II has more positive generation due to greater upward motion into the jet. Lastly, as with $\{4\}$, the sign of the generation changes at the jet level.

For the cross sections of $\{6\text{'s}\}$, the integrand evaluated is $\frac{2\pi}{g} a^2 \cos^2\phi \left\{[\bar{u}^*\bar{\omega}^*]+[\bar{u}^*\bar{\omega}^*]+[\bar{F}_r]\right\}\frac{\partial}{\partial P}\left\{\frac{[\bar{u}]}{a\cos\phi}\right\}$. This term represents the generation of mean zonal kinetic energy

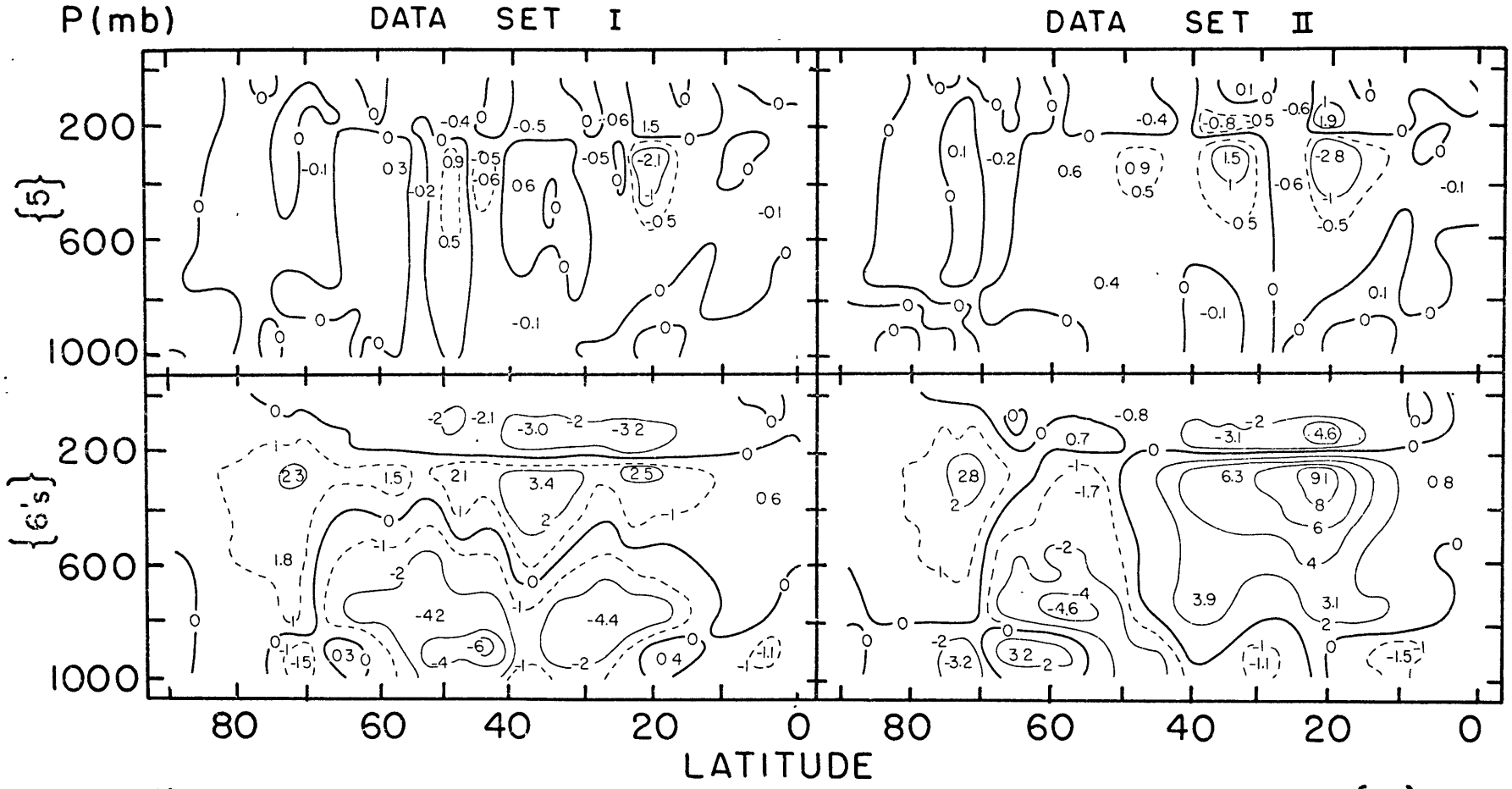


Fig. 11. Meridional cross sections of the internal vertical integrands $\{5\}$ and $\{6's\}$ in units of $10^6$ cm$^2$ sec.$^{-1}$

by the transport of relative momentum with or against the vertical gradient of angular velocity by vertical eddies of all types and scales. It is contained in both formulations of the ZKE equation and is normally one of the major terms in the ZKE balance for either equation.

Both data sets show the same reversal of sign at the jet stream level that characterized terms {4} and {5}. The generation above the jet is negative because of upward eddy momentum transports. The remainder of the cross sections below the jet are very similar to those for the vertical eddy transports of momentum in Figure 6, with upwards transports producing positive generation and downwards ones negative generations. Positive maxima in mid-latitudes below the jet are $3.4 \times 10^{6}$ cm $sec^{-1}$ at 37S and $9.1 \times 10^{6}$ at 23S, for sets I and II respectively. The negative maxima in the lower layers are $-6.0 \times 10^{6}$ at 45S and $-4.6 \times 10^{6}$ at 59S, for sets I and II respectively. These values merely reflect the greater upward transports of set II and the greater downward transports of set I. The positive generation near the surface around 60-65S where there are dowwnward transports of vertical eddy momentum, and the negative generation near the surface around 70-75S where there are upwards transports, are both caused by a reversal of the vertical gradient of angular velocity associated with the easterly jet over the Antartic at about 850 mb,

and for set II, in particular, with the anomalous surface westerlies in the Antartic.

3. Vertical boundary processes at $\phi = \phi_1$.

By now the interested reader is hopefully aware of the manner in which the integrands evaluated are to be interpreted. The boundary integrands are quite similar to the internal integrands, with only the actual value of the angular velocity substituted for the gradient of angular velocity. For the most part, the same basic mechanisms that are responsible for the spatial distributions and magnitudes of the internal integrands are likewise responsible for those of the boundary integrands. Therefore, in this section and in the next one, I will only present the definitions of each term and a brief summary of each group of boundary integrands, vertical and horizontal.

Figure 12 contains the meridional cross sections of integrands $\{7\}$ and $\{8\}$, and Figure 13 of $\{9'\}$ and $\{9''\}$. One thing should be made clear concerning these cross sections. A transport of momentum which is negative, i.e. poleward, corresponds to a transport of zonal kinetic energy through the latitude wall into the polar cap if the zonal wind is westerly. In other words, if the integrand is negative it contributes in a positive sense to the ZKE balance. On the cross sections the signs have already been changed so as to indicate whether the polar

cap is gaining or losing ZKE. As discussed in Chapter III, the vertical boundary integrals are the only ones that have a minus sign in front of the integral when written in pressure co-ordinates. What has been done on the cross sections for this group is to take the minus sign into the integrand for the sake of clarity.

For the cross sections of $\{7\}$, the integrand evaluated is $(-)\ \frac{2\pi}{g} a^2 \cos^2\phi\, (\Omega a \cos\phi)\, [\bar{v}]_m \frac{[\bar{u}]}{a\cos\phi}$. This term represents the horizontal transport of mean zonal kinetic energy through work done by the stress component associated with the rotation of the earth, $\Omega$, acting across the vertical surface at $\phi_1$. It is contained in the symmetric formulation of the ZKE equation only, and may be significant in the ZKE balances of some polar caps.

For the cross sections of $\{8\}$, the integrand evaluated is $(-)\ \frac{2\pi}{g} a^2 \cos^2\phi\, [\bar{u}]\, [\bar{v}]_m \frac{[\bar{u}]}{a\cos\phi}$. This term represents the horizontal transport of mean zonal kinetic energy through work done by the stress component associated with the relative rotation, $[\bar{u}]$, acting across the vertical surface at $\phi_1$. It is contained in both formulations of the ZKE equation and is normally not a major term in the ZKE balances for most polar caps for either equation.

For the cross sections of $\{9'\}$, the integrand evaluated is $(-)\ \frac{2\pi}{g} a^2 \cos^2\phi\, [\bar{u}^*\bar{v}^*] \frac{[\bar{u}]}{a\cos\phi}$.

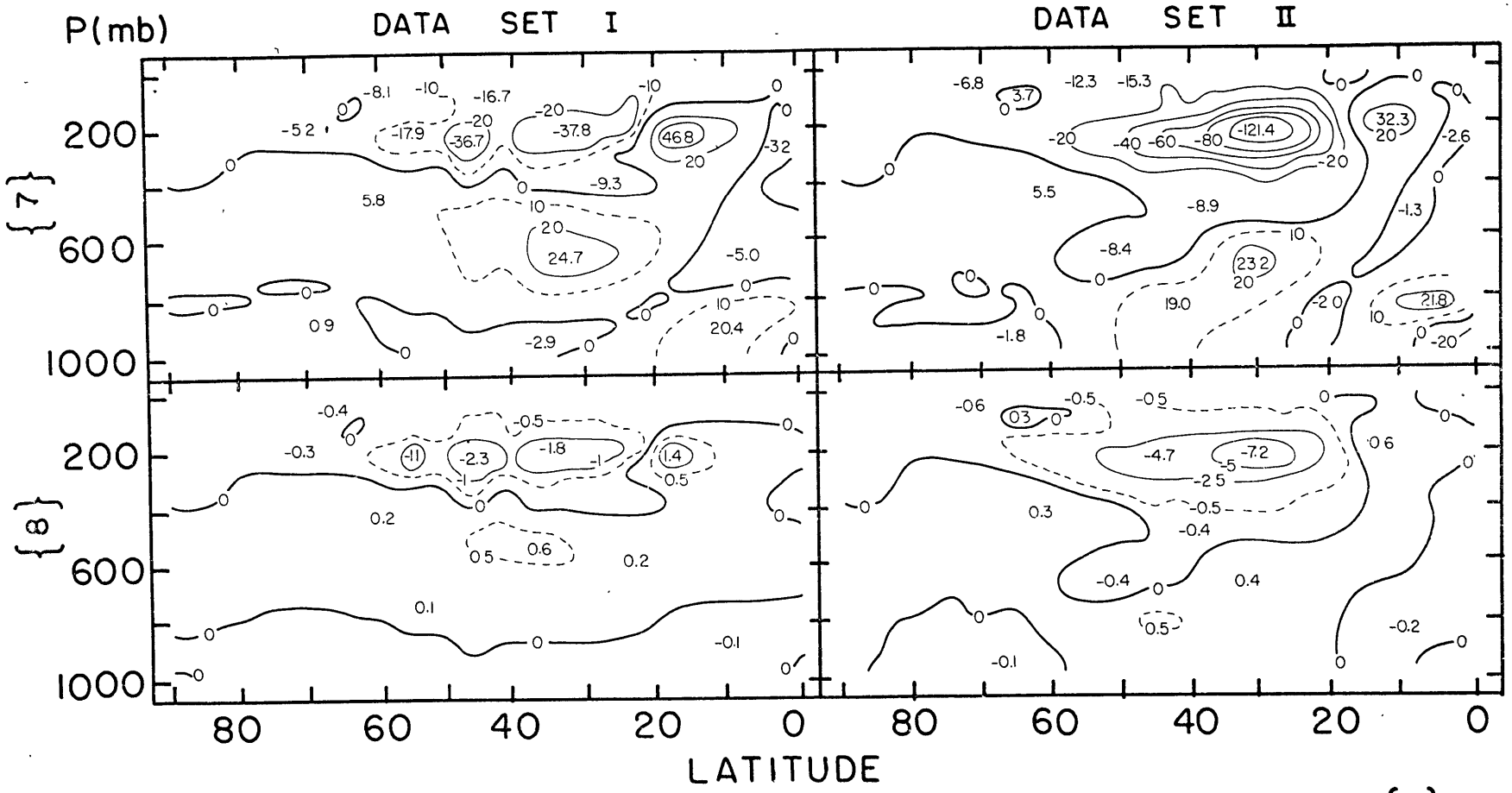


Fig. 12. Meridional cross sections of the vertical boundary integrands {7} and {8} in units of $10^{14}$ cm$^3$ sec$^{-1}$.

This term represents the horizontal transport of mean zonal kinetic energy through work done by the stress component associated with the standing eddy motion, $\bar{u}^*$, acting across the vertical surface at $\phi_1$. It is contained in both formulations of the ZKE equation and is not normally a major term in the ZKE balances for most polar caps for either equation.

For the cross sections of $\{9''\}$, the integrand evaluated is $(-)\frac{2\pi}{g} a^2 \cos^2\phi [\bar{u}^*\bar{v}^*] \frac{[\bar{u}]}{a\cos\phi}$. This term represents the horizontal transport of mean zonal kinetic energy through work done by the stress component associated with the transient eddy motion, $u'$, acting across the vertical surface at $\phi_1$. It is contained in both formulations of the ZKE equation and may be significant in the ZKE balances of some polar caps for either formulation.

Terms $\{8\}$ and $\{9'\}$ are generally quite negligible for all latitude wall boundaries. Terms $\{7\}$ and $\{9''\}$ are important at some latitude walls, particularly in low to middle latitudes. Term $\{7\}$ has large equatorwards transports of ZKE in both data sets in mid-latitudes at the jet level due to the upper level southerlies of the indirect cells. This effect is much more pronounced for set II as expected from previous discussions. There are significant poleward transports below these due to the lower

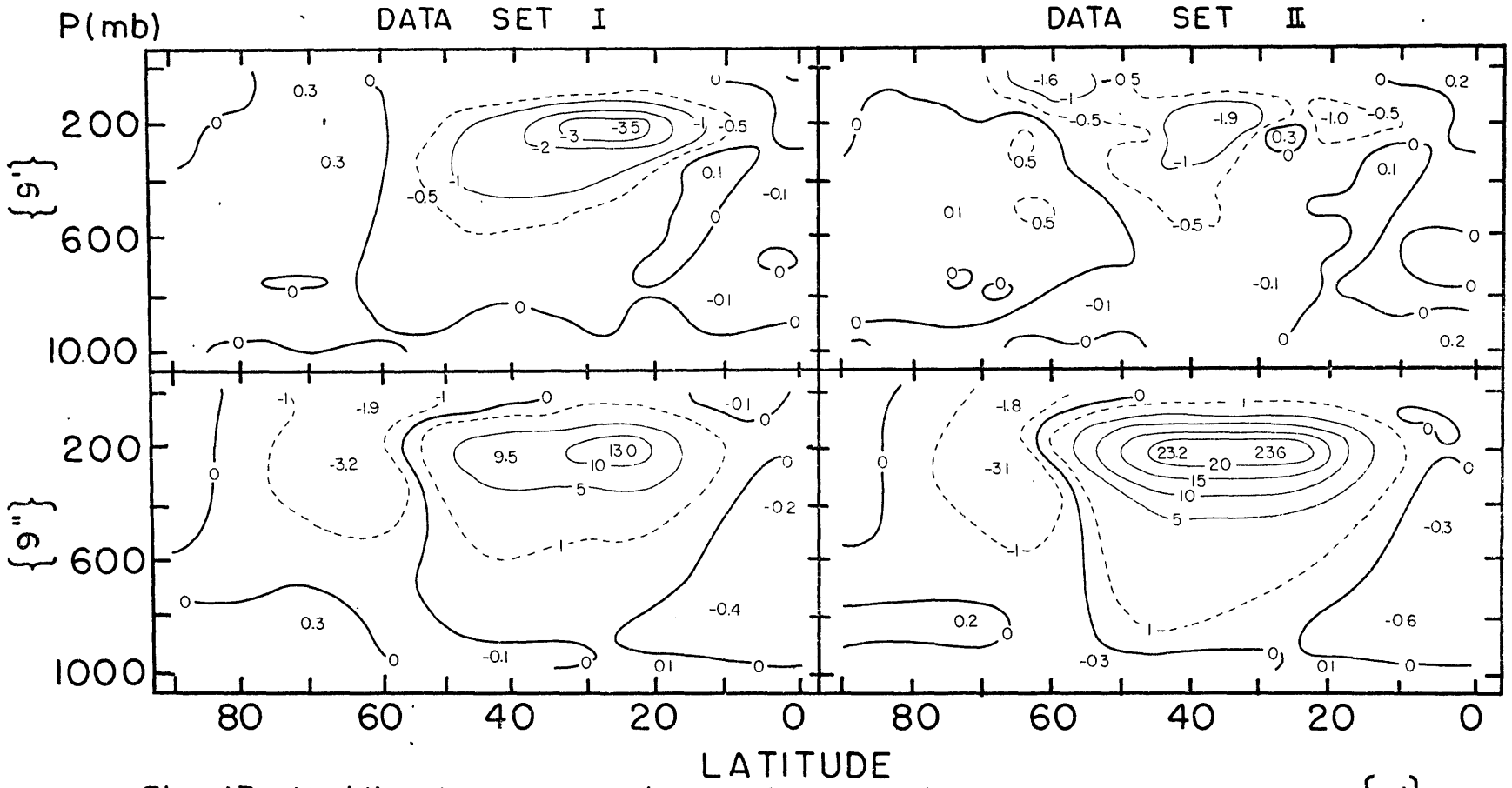


Fig. 13. Meridional cross sections of the vertical boundary integrands $\{9'\}$ and $\{9''\}$ in units of $10^{14}$ cm$^3$ sec$^{-1}$

level northerlies, and compensation in the vertical may therefore occur for some latitude walls. However, the high levels usually dominate. At low latitudes, for both data sets, there are poleward transports at both high and low levels due to the upper level northerlies of the Hadley Cell acting on westerly winds and the lower level southerlies acting on easterly winds. The low latitude phenomenon is more important for set I, as expected. For $\{9''\}$, there are significant poleward transports throughout mid-latitudes, especially for set II. This is hardly surprising considering the cross sections of transient eddy momentum transports in Figure 5. Compensation between high and low levels is not a factor for $\{9''\}$. When considering the entire hemispheric volume, the transports of ZKE via all four terms across the equatorial latitude wall are of minor importance in the ZKE balance. For further details of these transports and those across various other latitude walls, see section 6 of this chapter.

4. Horizontal boundary processes at $P = P_1$.

Figure 14 contains the meridional cross sections of integrands $\{10\}$, $\{11\}$ and $\{12's\}$.

For the cross sections of $\{10\}$, the integrand evaluated is $\frac{2\pi}{g} a^2 \cos^2\phi \, (\Omega a \cos\phi)[\bar{\omega}] \frac{[\bar{u}]}{a\cos\phi}$. This term represents the vertical transport of mean zonal kinetic energy through work done by the stress component

associated with the rotation of the earth, $\Omega$, acting across the horizontal surface at $P_1$. It is contained in the symmetric formulation of the ZKE equation only and may be significant in the ZKE balances of some polar caps.

For the cross sections of $\{11\}$, the integrand evaluated is $\frac{2\pi}{g} a^2 \cos^2\phi [\bar{u}] [\bar{\omega}] \frac{[\bar{u}]}{a\cos\phi}$. This term represents the vertical transport of mean zonal kinetic energy through work done by the stress component associated with the relative motion, $[\bar{u}]$, acting across the horizontal surface at $P_1$. It is contained in both formulations of the ZKE equation and is not a major term in the ZKE balances of any polar caps for either formulation.

For the cross sections of $\{12's\}$, the integrand evaluated is $\frac{2\pi}{g} a^2 \cos^2\phi \left\{[\bar{u}'\bar{\omega}'] + [\bar{u}^*\bar{\omega}^*] + [\bar{\tau}_F]\right\} \frac{[\bar{u}]}{a\cos\phi}$. This term represents the vertical transport of mean zonal kinetic energy through work done by the stress component associated with eddy motions of all types and scales acting across the horizontal surface at $P_1$. It is contained in both formulations of the ZKE equation and may be important in the ZKE balances of some polar caps for either formulation.

On the cross sections for this group, downward transports are into the polar cap and therefore positive. Term $\{11\}$ is quite negligible for all polar caps. Terms $\{10\}$ and $\{12's\}$ may be important in the ZKE balances of some

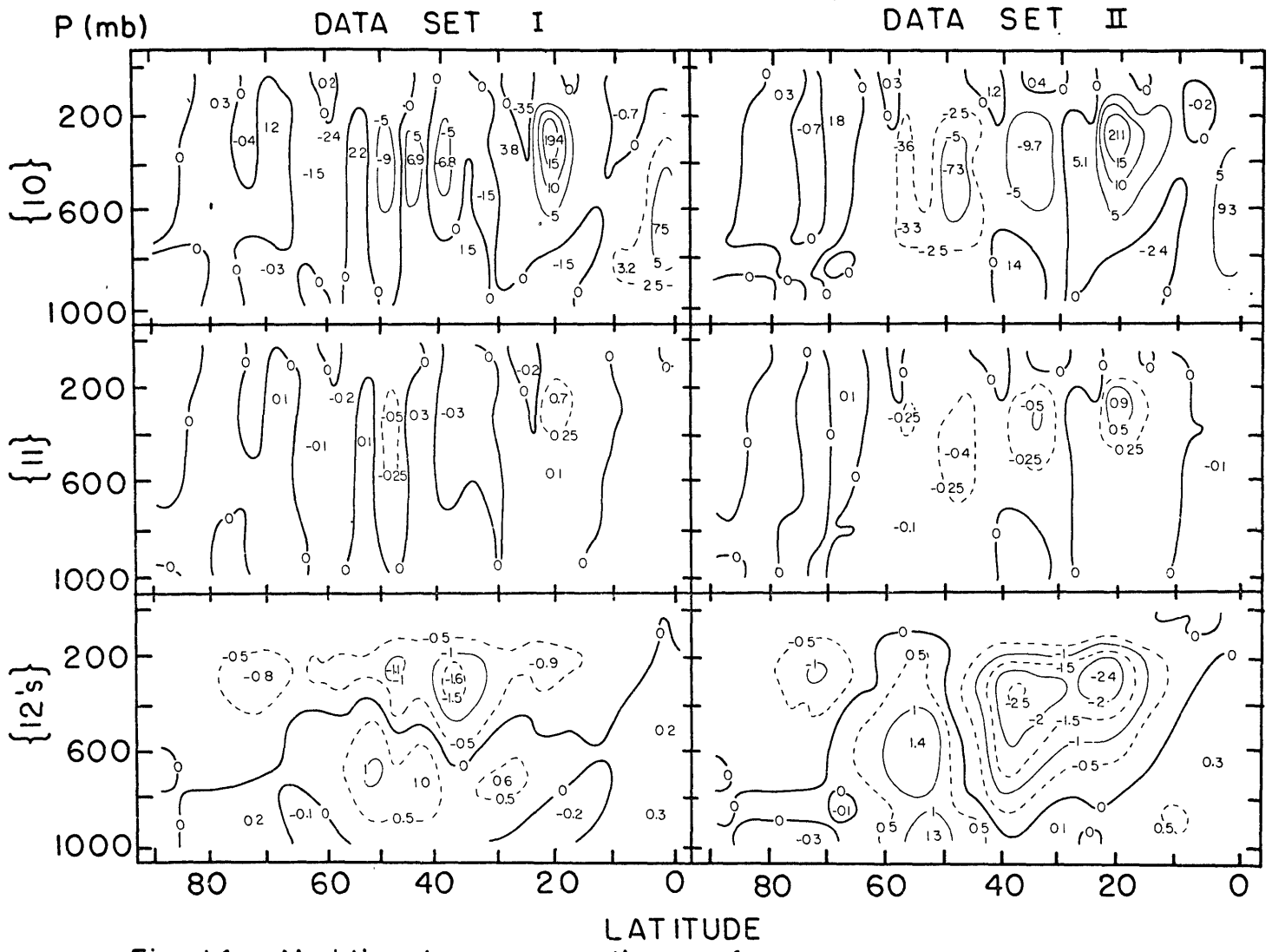


Fig. 14. Meridional cross sections of the horizontal boundary integrands {10}, {11} and {12's} in units of $10^{12}$ erg $cm^{-1}$ $sec^{-1}$.

polar caps. For $\{10\}$, in both data sets, there are downward transports of ZKE near the equator in mid-levels associated with the rising branch of the Hadley Cell acting on easterly winds. Largest transports are just below the jet around 20S and are downward because of the descending branches of the Hadley and Ferrel Cells acting on westerlies. This effect is somewhat greater for set II. In middle latitudes there are significant upward transports, especially for set II, due to rising motion in the indirect cells. There is therefore compensation between high and low latitudes along some upper bounding surfaces, but the low latitude transports would usually dominate. For $\{12's\}$, the cross sections bear great resemblance to those for the vertical eddy transports of momentum in Figure 6. For data set I, transports across lower levels are for the most part downward, while those across upper levels are upward. Thus, compensation between high and low latitudes is not a factor here. For set II, there is generally upward transports across most levels from about 20 to 45S, and downward transports from 45 to 70S. Compensation between high and low latitudes is therefore important for most levels. The upward transports at the lower latitudes would seem to dominate. For the entire hemispheric volume, the transports of ZKE via all three terms across the upper bounding surface of $P_1$=13 mb are assumed to be zero. For further details of the transports

across various upper bounding surfaces, see section 6 of this chapter.

5. Mountain torque calculations.

Tables 6 and 7 are the results of the mountain torque calculations for data sets I and II respectively. The method of calculation is that described in Chapter III. It should be noted that the effect in the 85 - 90S latitude band is unknown. However, it is doubtful that this has much effect on our results since $\tau_x$ is probably quite small in this band.

A few words about the hemispheric results. We would expect the mountain torque term to be smaller in the S. Hemisphere than in the N. Hemisphere due to the greater amount of area covered by ocean in the S. Hemisphere. This is confirmed by our results. The N. Hemisphere value is $-.55 \times 10^{20}$ erg $sec^{-1}$, as compared to $-.30 \times 10^{20}$ for data set I and $-.48 \times 10^{20}$ for data set II. It is interesting to note that the mountain torque acts in the same manner in both hemispheres, i.e. to destroy mean zonal kinetic energy. Data set II has a greater magnitude than data set I because of the stronger winds of the former. In fact, the circulation is so much stronger for this data set that it almost compensates for the greater amount of mountains in the N. Hemisphere, and the torque term is only slightly less than that for the N. Hemisphere.

Table 6. Mountain torque calculations for data set I.

| Latitude | $\tau_x$ ($10^{25}$erg) | $\frac{[\bar{u}]}{a\cos\phi}$ ($10^{-7}$sec$^{-1}$) | MT ($10^{18}$erg sec$^{-1}$) |
|---|---|---|---|
| 85-90S | ------- | -4.80 | --------- |
| 80-85 | .03 | -4.80 | -.14 |
| 75-80 | .07 | -5.03 | -.35 |
| 70-75 | .15 | -9.23 | -1.38 |
| 65-70 | .10 | -8.25 | -.83 |
| 60-65 | .00 | -.74 | .00 |
| 55-60 | .00 | 4.61 | .00 |
| 50-55 | -.11 | 9.00 | -.99 |
| 45-50 | -.43 | 10.48 | -4.51 |
| 40-45 | -.71 | 9.78 | -6.94 |
| 35-40 | -.85 | 7.48 | -6.36 |
| 30-35 | -.96 | 4.16 | -3.99 |
| 25-30 | -.71 | 1.59 | -1.13 |
| 20-25 | -.09 | -1.44 | .13 |
| 15-20 | -.03 | -3.46 | .10 |
| 10-15 | -.10 | -4.84 | .48 |
| 5-10 | .35 | -4.69 | -1.64 |
| 0-5 | .64 | -4.10 | -2.62 |
| | | | -30.17 |

Table 7. Mountain torque calculations for data set II.

| Latitude | $\tau_x$ ($10^{25}$erg) | $\frac{[\Delta m]}{a \cos\phi}$ ($10^{-7}$sec$^{-1}$) | MT ($10^{18}$erg sec$^{-1}$) |
|---|---|---|---|
| 85-90S | --------- | -5.10 | ---------- |
| 80-85 | .03 | -5.10 | -.15 |
| 75-80 | .07 | -5.13 | -.36 |
| 70-75 | .15 | -8.03 | -1.20 |
| 65-70 | .10 | -4.68 | -.47 |
| 60-65 | .00 | 6.48 | .00 |
| 55-60 | .00 | 14.05 | .00 |
| 50-55 | -.11 | 19.26 | -2.12 |
| 45-50 | -.43 | 19.91 | -8.56 |
| 40-45 | -.71 | 16.56 | -11.76 |
| 35-40 | -.85 | 12.09 | -10.28 |
| 30-35 | -.96 | 6.70 | -6.43 |
| 25-30 | -.71 | 2.90 | -2.06 |
| 20-25 | -.09 | -1.20 | .11 |
| 15-20 | -.03 | -3.80 | .11 |
| 10-15 | -.10 | -5.46 | .55 |
| 5-10 | .35 | -5.39 | -1.89 |
| 0-5 | .64 | -4.78 | -3.06 |
| | | | -47.57 |

6. Balance of ZKE.

In this section, the balances of ZKE for various size polar caps are presented. The ZKE balance equation is a closed one, with all the vertical processes deduced from horizontal processes via conservation of mass and angular momentum. That is to say, if we allow for the action of mountain torques the balance should ideally be zero, assuming that the atmosphere is neither gaining nor losing ZKE. The latter is a reasonable assumption since we are dealing with a five-year period. However, in most instances there is a small remainder left after all the terms in the equation have been summed. The remainders are usually called residuals. An explanation for these residuals is not easy to pin down. But, it is assumed that they probably reflect the quality of the data. More will be said about possible causes of residuals at the end of this section.

As previously discussed, the balances for two types of polar caps were evaluated. First, there are polar caps of fixed height (presumably from the ground to the "top" of the atmosphere) and increasing latitudinal extent. This is the Sims method. Results for this method are presented in Tables 8 and 9. Second, there are polar caps of fixed latitudinal extent (from pole to equator) and increasing depth. This is the Rosen method. Tables 10 and 11 present the results for this method. Each table

presents the evaluation for both the symmetric and traditional formulations. The row "RES" refers to the residuals of the former, and the row "RES'" to those of the latter.

It should be reiterated that the lower boundary is taken to be a smooth earth at 1013 mb, and the top of the atmosphere at 13 mb. These assumptions do introduce some error. The assumption at the ground is most likely less valid and of more consequence than the one at the top. Mountain torque calculations previously presented are included in an effort to partially correct for the lower boundary assumptions. For the Sims method, it was possible to evaluate the mountain torque term ("MT" in the tables) for each polar cap considered since the torques available from Newton were already calculated for latitude bands. This was not possible for the Rosen method for obvious reasons. This fact is only significant for polar caps with upper boundaries close to the ground. For polar caps whose upper boundaries clear all the mountains no error is introduced. Because the calculation for the mountain torque term represents at best only a fair estimate of the actual physical phenomenon, it is probably already in error by an amount just as large as the one introduced by using the same value for it for polar caps of all depths.

Obviously, there is a wealth of detailed information contained in the four tables. I shall not discuss the

balance for each particular cap, but will restrict myself to the more important features of each table. Since the equation is almost forced to balance, the residuals are not really the main object of interest, although they may reflect certain features of the data sets, processes of evaluation, or mathematical formulations. Rather, the important thing is to consider which terms contribute significantly to the equation. Which terms do so is not so forced by mathematical considerations and these terms are hoped to reflect the real nature of the physical processes that maintain the general circulation.

One fact is immediately evident. The residuals for data set I are much smaller than those for set II. Hemispheric values for set I are $.17 \times 10^{20}$ erg sec$^{-1}$ for RES and $-.38 \times 10^{20}$ for RES'. The values for set II are $+2.41 \times 10^{20}$ and $+1.68 \times 10^{20}$ respectively. As was true for the values of the vertical averages of $[\overline{\omega}]$, this would seem to indicate that data set I, without the bogus stations, is a more reliable data set. In fact, the very small residuals for this set are quite amazing.

Table 8 has the results for the Sims method for data set I. In general, the residuals for both formulations show the same variation with volume, being about zero for the smaller polar caps, then becoming more negative with maxima for the polar cap with the latitude wall at 20S of

$-.67 \times 10^{20}$ and $-.66 \times 10^{20}$ erg sec$^{-1}$ for RES and RES' respectively, and then becoming more positive for the largest volumes. For the hemispheric volume, it appears that the symmetric formulation gives a better result than the traditional. In the N. Hemisphere studies (see Rosen, 1970, Sims, 1969, and Starr et. al., 1970) the opposite was found. The only differences between the two formulations are in those terms containing $\Omega$. For the Sims method, where all transports across the upper boundary $\{10\}$, $\{11\}$, and $\{12\text{'s}\}$ are assumed to be zero, this means that the sum $\{1\} + \{4\} + \{7\}$ in the symmetric scheme should equal $\{1'\} + \{4'\}$ in the traditional scheme. For the hemispheric volume the former equals $.98 \times 10^{20}$ erg sec$^{-1}$ and the latter $.43 \times 10^{20}$. Since the $\Omega$ terms in the symmetric formulation are dependent on the very large term $(\Omega a \cos\phi)$ which multiplies any errors inherent in the evaluation of $[\bar{v}]$ and hence $[\bar{\omega}]$ as previously discussed, it had been assumed that the traditional scheme would balance better. It should be noted, however, that since both RES and RES' are so small in Table 8, one cannot really state which data set is more reliable on the basis of whether RES or RES' is smaller.

The important terms in the symmetric scheme are $\{1\}$, $\{3''\}$, $\{4\}$ and $\{6\text{'s}\}$ particularly for the hemispheric balance. $\{1\}$ and $\{4\}$ are very large and nearly balance each other, with hemispheric values of $18.60 \times 10^{20}$ erg sec$^{-1}$

Table 8. Balance of mean zonal kinetic energy for polar caps of increasing latitudinal extent (Sims method) for data set I. Units are $10^{20}$ erg $sec^{-1}$.

| 90S to | 80 | 70 | 60 | 50 | 40 | 30 | 20 | 10 | 0S |
|---|---|---|---|---|---|---|---|---|---|
| {1} | .00 | -.01 | -.26 | -.74 | -1.18 | .41 | 2.90 | 13.40 | 18.60 |
| {2} | .00 | .00 | -.02 | -.03 | -.06 | -.05 | -.04 | .11 | .11 |
| {3'} | .00 | .00 | .00 | .01 | -.07 | -.25 | -.51 | -.70 | -.74 |
| {3"} | .00 | .02 | .21 | .22 | .51 | 1.07 | 2.27 | 3.48 | 3.63 |
| {4} | -.03 | -.23 | .13 | .84 | .06 | .29 | -10.30 | -18.50 | -17.80 |
| {5} | .00 | .00 | .01 | .03 | .03 | .06 | -.11 | -.18 | -.19 |
| {6's} | .30 | 1.21 | .90 | -.57 | -1.75 | -2.23 | -3.16 | -3.22 | -3.27 |
| {7} | -.14 | -.10 | .06 | -.32 | .54 | -1.42 | 6.83 | 6.08 | .18 |
| {8} | -.01 | -.03 | -.04 | -.08 | -.06 | -.19 | .12 | .01 | .00 |
| {9'} | .01 | .09 | -.01 | -.41 | -.59 | -.74 | -.44 | -.06 | .00 |
| {9"} | -.11 | -.85 | -.97 | .94 | 2.34 | 2.69 | 2.04 | .03 | -.05 |
| MT | .00 | -.02 | -.03 | -.04 | -.15 | -.25 | -.27 | -.26 | -.30 |
| RES | .02 | .08 | -.02 | -.15 | -.38 | -.61 | -.67 | .19 | .17 |
| {1'} | -.18 | -.38 | -.05 | -.13 | -.48 | -.60 | -.56 | .32 | .41 |
| {4'} | .00 | .00 | .00 | .00 | .00 | .00 | .00 | .01 | .02 |
| RES' | .01 | .04 | .00 | -.06 | -.28 | -.49 | -.66 | -.46 | -.38 |

and $-17.80 \times 10^{20}$ erg $sec^{-1}$ respectively. $\{3''\}$ and $\{6's\}$ also very nearly balance, with values of $3.63 \times 10^{20}$ and $-3.27 \times 10^{20}$. The latter corresponds to a balance between generation by horizontal transient eddy momentum transports and destruction by vertical eddy momentum transports. That $\{3''\}$ generates ZKE is not surprising from the cross section of the integrand of this term. The destruction of ZKE by the vertical eddies indicates that the action of downward transports of momentum in the lower half of the atmosphere dominates over the upward transports above.

As pertains to the variation of the main terms with polar cap size the following is noted. $\{1\}$ is generally small but increasingly negative as the latitude wall moves from 80S to 40S. Maximum is $-1.18 \times 10^{20}$ erg $sec^{-1}$ for $\phi_1 =$ 40S. The increased magnitudes are partially due to the $\cos\phi$ dependence of $\{1\}$, as earlier noted. The values are negative because of the upper level southerlies in mid-latitudes. For the larger volumes, $\{1\}$ becomes increasingly positive due to the upper level northerlies of the Hadley Cell. The $\cos\phi$ dependence is quite obvious. Maximum value is the hemispheric value.

$\{3''\}$ is positive for all polar caps, increasing as the latitude wall moves toward the equator. This was expected from the cross section of the transient eddy transports of momentum. This term is significant for polar caps with

latitude walls from about 35S to the equator. Maximum value is the hemispheric one. $\{4\}$ is quite large and negative for polar caps extending to 20S, 10S and 0S. Maximum value is $-18.50 \times 10^{20}$ erg $sec^{-1}$ at 10S. Again, the $\cos\phi$ dependence is obvious. The large negative generation is due to the downward transports of $-\Omega$ -momentum in the descending branches of the Hadley Cell. $\{6's\}$ is positive for polar caps from 80S to 60S, with maximum of $1.21 \times 10^{20}$ at 70S. From 50S to the equator, $\{6's\}$ becomes increasingly negative. Maximum value is the hemispheric one again. At high latitudes upwards vertical eddy momentum transports dominate, but downward transports in the lower half of the atmosphere dominates over all upward transports as the polar cap increases in size.

Two of the vertical boundary processes are important for some of the polar caps. $\{7\}$ is large and positive for the latitude walls at 20S and 10S. Maximum value is $6.83 \times 10^{20}$ erg $sec^{-1}$ at 20S. These values are due primarily to the upper level northerlies of the Hadley Cell acting on westerly winds and the low level southerlies acting on easterlies. $\{9''\}$ is significant for latitude walls from 70S to 20S. Maximum negative value is $-.97 \times 10^{20}$ at 60S and maximum positive value is $2.69 \times 10^{20}$ at 30S. The latter reflects the strength of the polewards transient eddy transports north of the jet.

For the traditional scheme, $\{4'\}$ is totally insignificant. $\{1'\}$ is larger, but the main balance is between $\{3''\}$ and $\{6's\}$ for the hemispheric volume.

Table 9 has the results for the Sims method for data set II. As was true for set I, RES and RES' show identical variations as the latitude wall moves north. Down to 60S they are negative with maximum values at 70S. For the remaining polar caps they are positive with secondary maxima at 40S and primary maxima for the hemispheric volume. These residuals do not vary in the same manner as those of set I, and no physical explanation can readily be attached to the variations for either set. However, the maximum values being the hemispheric ones for set II would seem to indicate a particular imbalance in low latitudes. This could be attributed to the scarcity of data in the equatorial tropics. But this effect is not evident for set I. The hemispheric value of RES' is now smaller than that of RES and the argument concerning the $\Lambda$-terms could be invoked. The symmetric $\Lambda$-terms sum to $-9.66 \times 10^{20}$ erg $sec^{-1}$ and the traditional ones to $-10.39 \times 10^{20}$ for the hemispheric volume. It is interesting that the residuals are significantly positive rather than negative. This may indicate that our mathematical formulation may be quite in error near the lower boundary and does not detect much of the destruction of ZKE by surface friction.

The same four terms are involved in the hemispheric balance as were in set I. However, there are important differences in the manner in which these terms act. Rather than $\{1\}$ balancing $\{4\}$ and $\{3''\}$ balancing $\{6's\}$, we now have $\{1\} + \{3''\} + \{6's\}$ vs $\{4\}$ as follows: 3.96+8.21+ 5.38 vs -14.40.

$\{1\}$ is much smaller in magnitude in set II than in set I. The difference can be mainly attributed to the increased strength of the mid-latitude indirect cell with its upper level southerlies destroying ZKE and making $\{1\}$ much less positive than before. In fact, $\{1\}$ is now large and negative for polar caps with latitude walls from 50S to 20S, with a maximum of $-4.17 \times 10^{20}$ erg $sec^{-1}$ at 20S. The hemispheric value is positive because the $\cos\phi$ dependence allows the Hadley Cell to dominate over the indirect cell.

$\{3''\}$ is much larger than for set I, as expected, due to the greater polewards transient eddy momentum transports of set II. As with set I, it is increasingly positive as the polar cap increases in volume. The hemispheric value is the maximum. For term $\{4\}$, the important change from set I is the large positive magnitudes for polar caps with latitude walls from 50S to 30S. Maximum value is $12.80 \times 10^{20}$ erg $sec^{-1}$ at 30S. The corresponding maximum for set I is $.84 \times 10^{20}$ at 50S. This is again due

Table 9. Balance of mean zonal kinetic energy for polar caps of increasing latitudinal extent (Sims method) for data set II. Units are $10^{20}$ erg $sec^{-1}$.

| 90 S to | 80 | 70 | 60 | 50 | 40 | 30 | 20 | 10 | 0 S |
|---|---|---|---|---|---|---|---|---|---|
| {1} | .00 | .00 | -.32 | -.95 | -2.16 | -1.71 | -4.17 | -.12 | 3.96 |
| {2} | .00 | .00 | -.01 | -.04 | -.19 | -.34 | -.61 | -.56 | -.55 |
| {3'} | .00 | -.01 | -.09 | -.13 | -.23 | -.36 | -.45 | -.55 | -.59 |
| {3"} | .00 | .13 | .57 | .70 | 2.03 | 3.71 | 6.16 | 8.03 | 8.21 |
| {4} | -.06 | .01 | .64 | 4.00 | 7.18 | 12.80 | .30 | -16.10 | -14.40 |
| {5} | .00 | .00 | .02 | .18 | .33 | .54 | .30 | .15 | .14 |
| {6's} | .22 | .80 | .43 | -.92 | -.52 | 1.50 | 3.92 | 5.30 | 5.38 |
| {7} | -.13 | -.46 | -.92 | -5.05 | -9.80 | -19.40 | -6.87 | 6.42 | .78 |
| {8} | -.01 | -.06 | -.11 | -.49 | -.75 | -1.12 | -.24 | .01 | -.01 |
| {9'} | .01 | .02 | -.07 | -.29 | -.48 | -.19 | -.16 | -.03 | .03 |
| {9"} | -.12 | -.99 | -.46 | 3.93 | 6.17 | 5.97 | 3.36 | .05 | -.06 |
| MT | .00 | -.02 | -.02 | -.04 | -.25 | -.41 | -.43 | -.42 | -.48 |
| RES | -.09 | -.58 | -.34 | .90 | 1.33 | .99 | 1.11 | 1.18 | 2.41 |
| {1'} | -.19 | -.47 | -.59 | -1.94 | -4.69 | -8.05 | -10.70 | -10.50 | -10.40 |
| {4'} | .00 | .00 | .00 | -.01 | -.01 | -.02 | -.01 | .00 | .01 |
| RES' | -.09 | -.60 | -.33 | .95 | 1.41 | 1.23 | 1.14 | 1.48 | 1.68 |

to the overall stronger circulation of set II with strong rising motion counter-gradient to $\frac{[\bar{u}]}{a\cos\varphi}$ in the indirect cell. For set I, the effect is weak because the indirect cell at upper levels and the direct one at lower levels compensate for each other in the vertical in mid-latitudes. Back to set II, the values for $\{4\}$ are large and negative for the largest polar caps as was true for set I. Maximum value is $-16.10 \times 10^{20}$ erg sec$^{-1}$ for the polar cap extending to 20S. This is slightly less than the value for set I since that set has a stronger Hadley Cell.

The most significant change from set I concerns $\{6's\}$. We again have positive generation for latitude walls from 80S to 60S. But the strong negative generation of set I for the larger polar caps does not appear for set II. Instead there is large positive generation from 30S to the equator. Maximum value is the hemispheric one. The absolute value of the set II maximum is also much larger than that for set I. The only polar caps where downward transports of eddy momentum dominate are those with latitude walls extending to 50S and 40S. For the larger volumes, upward transports of momentum dominate.

As with set I, $\{7\}$ and $\{9''\}$ are quite important for some polar caps. $\{7\}$ is large and negative for latitude walls from 50S to 20S due to the upper level southerlies of the indirect cell. Maximum value is $-19.40 \times 10^{20}$ erg sec$^{-1}$

at 30S, the largest value on either Tables 8 or 9. This is quite a difference from set I where compensation in the vertical produces weak transports in middle latitudes. Note that where $\{7\}$ has its extreme value (negative) is where $\{4\}$ has its extreme value (positive). The balance for this polar cap is thus much different from the hemispheric one. The influence of the Hadley Cell is still apparent for term $\{7\}$ with the positive maximum of $6.42 \times 10^{20}$ at 10S. $\{9''\}$ is also larger for set II, with significant positive values from 50S to 20S. Maximum is $6.27 \times 10^{20}$ at 40S, just north of the jet maximum.

There is also a great change in the balance for the traditional scheme from set I to set II. Whereas $\{1'\}$ was not important for set I, it is now very important. It is large and negative for polar caps with latitude walls from 50S to 0S. Maximum value is $-10.70 \times 10^{20}$ erg $sec^{-1}$ for $\phi_1$ = 20S. The significant process here is the deflection of the strong upper level southerlies of the indirect cell toward the west via Coriolis forces thus decreasing the ZKE of the westerlies. The hemispheric value is $-10.40 \times 10^{20}$. The important terms in the hemispheric balance are now $\{3'\} + \{6's\}$ vs $\{1'\}$.

Table 10 presents the results for the Rosen method for data set I. The residuals do not vary with height of the upper boundary as smoothly as they did with the

placement of the variable latitude wall. It is interesting that the residuals are smaller for the traditional scheme except for the hemispheric volume. Again, this might be attributable to the different $\Omega$ -term formulations. Maximum RES is $+1.07 \times 10^{20}$ erg $sec^{-1}$ for the upper surface at 113 mb, and maximum RES' $-.38 \times 10^{20}$ which is the hemispheric value. These would seem to indicate significant imbalances in the uppermost layers of the atmosphere. As noted in the chapter concerning the data, the data at 100 mb and 50 mb are particularly scarce, and this could be the reason for the larger residuals for the larger volumes.

In previous N. Hemisphere studies (see Rosen,1970), the residuals up to the jet stream level were observed to be approximately constant with height of the upper boundary, thus implying that most of the residual was due to an imbalance in the lowest surface layer because the mathematical formulation at the ground was inaccurate. In particular, it was felt that much of the destruction of ZKE by surface friction was being omitted as was suggested earlier. This effect is difficult to discern for set I since the residuals are fairly small.

The last column in Table 10 is identical to that in Table 8 and the earlier discussion concerning the hemispheric balance of ZKE will not be repeated. The variation

Table 10. Balance of mean zonal kinetic energy for polar caps of increasing vertical extent (Rosen method) for data set I. Units are $10^{20}$ erg $sec^{-1}$.

| 1013 mb to | 913 | 813 | 713 | 613 | 513 | 413 | 313 | 213 | 113 | 13 |
|---|---|---|---|---|---|---|---|---|---|---|
| {1} | -1.37 | -1.53 | .50 | 5.04 | 9.20 | 11.50 | 12.20 | 17.90 | 21.60 | 18.60 |
| {2} | .00 | .00 | .02 | .05 | .09 | .12 | .11 | .17 | .17 | .11 |
| {3'} | .00 | .00 | .01 | -.01 | -.03 | -.08 | -.15 | -.39 | -.69 | -.74 |
| {3"} | .00 | .06 | .18 | .36 | .60 | .99 | 1.72 | 2.87 | 3.66 | 3.63 |
| {4} | -1.24 | -3.64 | -6.33 | -8.29 | -10.40 | -12.90 | -16.20 | -18.40 | -17.50 | -17.80 |
| {5} | .00 | .00 | -.01 | -.01 | -.02 | -.04 | -.11 | -.18 | -.17 | -.19 |
| {6's} | -1.02 | -2.36 | -3.79 | -4.46 | -4.57 | -3.99 | -2.88 | -1.81 | -2.73 | -3.27 |
| {7} | -.51 | .07 | .50 | .14 | -.10 | -.04 | .27 | .18 | .10 | .18 |
| {8} | .00 | .00 | .00 | .00 | .00 | .00 | .00 | .00 | .00 | .00 |
| {9'} | .01 | .00 | .00 | .00 | .00 | -.01 | -.02 | -.01 | .00 | .00 |
| {9"} | .00 | -.01 | -.02 | -.03 | -.04 | -.05 | -.06 | -.06 | -.05 | -.05 |
| {10} | 3.24 | 5.64 | 6.58 | 6.01 | 6.09 | 7.80 | 10.10 | 5.82 | -.58 | .00 |
| {11} | -.01 | -.01 | -.01 | -.03 | -.06 | -.01 | .14 | .10 | -.05 | .00 |
| {12's} | 1.05 | 2.09 | 2.66 | 1.67 | -.29 | -2.77 | -5.03 | -5.35 | -2.39 | .00 |
| MT | -.30 | -.30 | -.30 | -.30 | -.30 | -.30 | -.30 | -.30 | -.30 | -.30 |
| RES | -.15 | .01 | -.01 | .14 | .17 | .22 | -.21 | .54 | 1.07 | .17 |
| {1'} | .23 | .49 | 1.20 | 2.73 | 4.62 | 6.20 | 6.61 | 5.01 | 2.49 | .41 |
| {4'} | .00 | .00 | .00 | .01 | .01 | .01 | .01 | .02 | .02 | .02 |
| RES' | -.04 | -.04 | -.06 | -.02 | .01 | .07 | .04 | .07 | -.04 | -.38 |

with height of the upper bounding surface of the important terms will be discussed.

$\{1\}$ is significant and negative for polar caps with heights of 913 and 813 mb. Here the low level southerlies of the Hadley Cell is the predominant mechanism. For the larger polar caps $\{1\}$ is very large and positive, with a maximum of $21.60 \times 10^{20}$ erg $sec^{-1}$ for the polar cap extending to 113 mb. This is the largest value on any of the Tables 8 through 11. The cos $\phi$ dependence of this term and the strength of the upper level northerlies of the Hadley Cell produces the large positive generation.

$\{3''\}$ is not really important until we get to the larger volumes. This is not surprising since the transient eddy transports of momentum are maximum near the jet level. Maximum value is $3.66 \times 10^{20}$ erg $sec^{-1}$ for the upper surface at 113 mb. $\{4\}$ is negative and important for all polar caps, with a maximum of $-18.40 \times 10^{20}$ for $P_1$ = 213 mb. As previously discussed, downward motion with the gradient of angular velocity in the descending branch of the Hadley Cell is responsible for the large negative generation. $\{6's\}$ is also negative and important for all polar caps. Maximum is $-4.57 \times 10^{20}$ for $P_1$ = 513 mb. Downward transports of eddy momentum in the lower layers and upward transports above the jet dominate here.

The horizontal boundary terms are assumed to be zero

at $P_1$ = 13 mb. However, both $\{10\}$ and $\{12's\}$ are significant at most of the other boundaries. $\{10\}$ is large and positive for all polarcaps except the very largest. Maximum value is $10.10 \times 10^{20}$ erg $sec^{-1}$ for $P_1$ = 313 mb. Just as downward motion in the Hadley Cell dominated $\{4\}$, the same is true of $\{10\}$. $\{12's\}$ is positive for polar caps with upper boundaries up to 613 mb. Maximum positive value is $2.66 \times 10^{20}$ at 713 mb. It is negative for the higher bounding surfaces, with a maximum of $-5.35 \times 10^{20}$ at 113 mb. As mentioned so many times before, this is due to downward eddy momentum transports in the lower half of the atmosphere and upwards ones in the upper half.

For the traditional scheme, $\{1'\}$ is important for the polar caps with bounding surfaces from 713 mb to 113 mb. Maximum value is $6.61 \times 10^{20}$ erg $sec^{-1}$ for $P_1$ = 313 mb. This positive generation is due to the mid-level mid-latitude northerlies between the upper level indirect cell and the direct cell below. As we get to higher levels, the upper southerlies of the Hadley Cell almost negate all of the positive generation produced in the layers below.

Table 11 is the results for the Rosen method for data set II. Now both RES and RES' are more nearly constant with height of the upper boundary, indicating that most of the residual is indeed in the surface layer. If the residual for that layer is subtracted from the hemi-

spheric residual, RES is reduced from $+2.41 \times 10^{20}$ erg $sec^{-1}$ to $+.59 \times 10^{20}$, and RES' from $+1.68 \times 10^{20}$ to $-.48 \times 10^{20}$. RES' is consistently less than RES and the argument concerning the different formulations of the $\Omega$ -terms appears to give a reasonable explanation for this. Also, RES has a primary maximum of $+2.93 \times 10^{20}$ for the polar cap bounded by 113 mb, and RES' has a relative maximum of $+1.97 \times 10^{20}$ for the same polar cap and a primary maximum of $+2.55 \times 10^{20}$ for $P_1$ = 313 mb. These may again indicate a major effect of lack of data at some upper levels.

{1} is now significant and positive for all polar caps. Whereas it was dominated by the upper level northerlies of the Hadley Cell in set I, thus producing maximum positive values for the larger polar caps, now the lower level northerlies of the stronger mid-latitude cell seems to be a dominant feature. Evidently, these winds combined with the upper level northerlies of the Hadley Cell are sufficient to overcome the strong upper southerlies of the indirect cell, thus producing positive generation for all polar caps. Maximum value is at a lower level than that for set I, and is $11.80 \times 10^{20}$ erg $sec^{-1}$ for $P_1$ = 513 mb.

{3"} follows the same pattern as it did in set I except the magnitudes are greater as expected. The hemispheric value is the maximum. {4} is again large and negative and for the same reasons as stated for set I. Max-

Table 11. Balance of mean zonal kinetic energy for polar caps of increasing vertical extent (Rosen method) for data set II. Units are $10^{20}$ erg $sec^{-1}$.

| 1013 mb to | 913 | 813 | 713 | 613 | 513 | 413 | 313 | 213 | 113 | 13 |
|---|---|---|---|---|---|---|---|---|---|---|
| {1} | 1.99 | 4.96 | 8.12 | 11.20 | 11.80 | 10.80 | 7.97 | 5.32 | 5.68 | 3.96 |
| {2} | .02 | .05 | .09 | .13 | .13 | .09 | -.04 | -.33 | -.48 | -.55 |
| {3'} | -.01 | -.01 | -.03 | -.07 | -.13 | -.17 | -.21 | -.31 | -.48 | -.59 |
| {3"} | -.02 | .17 | .51 | .97 | 1.54 | 2.40 | 3.93 | 6.26 | 7.95 | 8.21 |
| {4} | -.49 | -1.25 | -2.52 | -4.12 | -6.52 | -9.91 | -13.70 | -16.50 | -14.70 | -14.40 |
| {5} | .00 | .01 | .07 | .12 | .18 | .19 | .18 | .13 | .14 | .14 |
| {6's} | -.59 | -.81 | -.71 | -.22 | .80 | 2.48 | 4.77 | 6.53 | 5.69 | 5.38 |
| {7} | -3.00 | -2.41 | -1.30 | -.90 | -.45 | .05 | .58 | .65 | .59 | .78 |
| {8} | .02 | .01 | .00 | .00 | .00 | .00 | .00 | .00 | .00 | -.01 |
| {9'} | .02 | .02 | .02 | .02 | .02 | .02 | .02 | .02 | .03 | .03 |
| {9"} | .00 | -.01 | -.02 | -.04 | -.05 | -.07 | -.08 | -.07 | -.07 | -.06 |
| {10} | 1.78 | .69 | -1.23 | -2.50 | -.95 | 3.07 | 7.42 | 6.62 | .90 | .00 |
| {11} | -.05 | -.11 | -.29 | -.46 | -.54 | -.46 | -.28 | -.05 | -.02 | .00 |
| {12's} | 2.63 | 1.44 | .09 | -1.20 | -3.01 | -5.64 | -7.66 | -5.61 | -1.82 | .00 |
| MT | -.48 | -.48 | -.48 | -.48 | -.48 | -.48 | -.48 | -.48 | -.48 | -.48 |
| RES | 1.82 | 2.27 | 2.32 | 2.45 | 2.34 | 2.37 | 2.38 | 2.18 | 2.93 | 2.41 |
| {1'} | .62 | 1.98 | 3.02 | 3.44 | 3.77 | 3.93 | 2.40 | -4.16 | -8.50 | -10.40 |
| {4'} | .00 | .00 | .00 | .00 | .00 | .00 | .00 | .00 | .01 | .01 |
| RES' | 2.16 | 2.26 | 2.27 | 2.21 | 2.23 | 2.29 | 2.55 | 1.93 | 1.97 | 1.68 |

imum is $-16.50 \times 10^{20}$ erg $sec^{-1}$ for the upper boundary at 213 mb. The magnitudes of $\{4\}$ are somewhat less than those for set I due to rising motion in the stronger indirect cell compensating for some of the downward motion in the descending branches of the Hadley and Ferrel Cells. The same change we saw in $\{6's\}$ from set I to set II in the Sims method is also apparent in the Rosen method. The generations are no longer consistently negative, but weakly negative for polar caps with bounding surfaces to 613 mb and strongly positive for the larger volumes. Maximum is $6.53 \times 10^{20}$ for $P_1$ = 213 mb.

For the horizontal boundary terms, $\{10\}$ and $\{12's\}$, there are also differences between the data sets. $\{10\}$ now has negative values for upper surfaces from 713 mb to 513 mb, with upward motion in the indirect cell dominating. Downward motion in the descending branches of the Hadley and Ferrel Cells still dominates for the polar caps extending from 413 mb to 113 mb. Maximum value is $7.42 \times 10^{20}$ erg $sec^{-1}$ at 313 mb, less than the maximum for set I. For $\{12's\}$, there are more negative transports of ZKE at more pressure levels due to the greater upwards transports of eddy momentum of set II. Maximum positive transport of ZKE is $2.63 \times 10^{20}$ for the surface layer; maximum negative transport is $-7.66 \times 10^{20}$ at 313 mb, just below the jet.

For the traditional scheme, $\{1'\}$ has also changed

character. It is no longer positive for all polar caps due to the strength of the upper southerlies of the indirect cell overcoming and dominating over the upper northerlies of the Hadley Cell and low level northerlies of the indirect cell. The latter accounts for most of the positive generation in the smaller polar caps. Maximum positive value is $3.93 \times 10^{20}$ erg $sec^{-1}$ for the polar cap bounded by 413 mb; maximum negative value is the hemispheric one.

The Rosen method gives one a good opportunity to look at the cross equatorial transports since the latitude wall is always at the equator. For both data sets, $\{8\}$, $\{9'\}$ and $\{9''\}$ are quite negligible for all depths. Of these three terms $\{9''\}$ is the largest. It is interesting that the negative hemispheric values for $\{9''\}$ indicate a transport of ZKE from the S. Hemisphere to the N. Hemisphere. In the N.Hemisphere study of Rosen, 1970, the opposite was found. The apparent disagreement is not so surprising considering the very small numbers involved.

$\{7\}$ is by far the largest transport term at the equator. Hemispheric values are $.18 \times 10^{20}$ erg $sec^{-1}$ and $.78 \times 10^{20}$ for sets I and II respectively. In set II, $\{7\}$ is significantly negative for polar caps with lower bounding surfaces. Maximum is $-3.00 \times 10^{20}$ for the polar cap extending to 913 mb. For the larger polar caps it is

positive. The positive hemispheric value for set I corresponds to the S. Hemisphere Hadley Cell bulging slightly across the equator. This is rather difficult to see on the cross section for $\psi$ in Figure 3, but the cross section for $[\overline{v}]_m$ on the same figure shows the situation more clearly. At low levels, southerly winds are transporting easterly momentum out of the S. Hemisphere, thus increasing the ZKE of the westerlies. At high levels, the northerlies accomplish the opposite. However, the action at low levels dominates. For data set II, the situation is more complicated. As seen on the cross section for $\psi$ , the N. Hemisphere Hadley Cell is bulging slightly across the equator at low to middle levels. The northerlies near the surface produce negative values for $\{7\}$ . However, this is compensated for throughout middle levels as the rising branch of the N. Hemisphere Hadley Cell slopes back across the equator toward the north, producing southerly winds and a positive value for $\{7\}$.

By way of summary, see Tables 12 and 13 for examples of significant balances for polar caps with various latitude walls and upper bounding surfaces. On these tables, when terms contribute in a positive sense they are listed on the left, and when they contribute in a negative sense they are listed on the right. The tables are designed to afford one an opportunity to more easily compare results for the symmetric and traditional formulations, and for

Table 12. Examples of significant balances of ZKE for polar caps with various latitude walls (Sims method). Units are $10^{20}$ erg $sec^{-1}$.

| 90S to | {1} | {3"} | {4} | {6's} | {7} | {9"} vs | {1} | {4} | {6's} | {7} | {8} |
|---|---|---|---|---|---|---|---|---|---|---|---|
| | | | | | | SYMMETRIC EQUATION | | | | | |
| | | | | | | DATA SET I | | | | | |
| 40 | . | . | . | . | . | 2.34 | -1.18 | . | -1.75 | . | . |
| 30 | . | 1.07 | . | . | . | +2.69 | . | . | -2.23 | -1.42 | . |
| 20 | 2.90 | +2.27 | . | . | +6.83 | +2.04 | . | -10.30 | -3.16 | . | . |
| 10 | 13.40 | +3.48 | . | . | +6.08 | . | . | -18.50 | -3.22 | . | . |
| 0 | 18.60 | +3.63 | . | . | . | . | . | -17.80 | -3.27 | . | . |
| | | | | | | DATA SET II | | | | | |
| 40 | . | 2.03 | +7.18 | . | . | +6.17 | -2.16 | . | . | -9.80 | . |
| 30 | . | 3.71 | +12.80 | +1.50 | . | +5.97 | -1.71 | . | . | -19.40 | -1.12 |
| 20 | . | 6.16 | . | +3.92 | . | +3.36 | -4.17 | . | . | -6.87 | . |
| 10 | . | 8.03 | . | +5.03 | +6.42 | . | . | -16.40 | . | . | . |
| 0 | 3.96 | +8.21 | . | +5.38 | . | . | . | -14.40 | . | . | . |
| | | {3"} | | {6's} | | {9"} vs | {1} | | {6's} | | {8} |
| | | | | | | TRADITIONAL EQUATION | | | | | |
| | | | | | | DATA SET I | | | | | |
| 40 | . | . | . | . | . | 2.34 | . | . | -1.75 | . | . |
| 30 | . | 1.07 | . | . | . | +2.69 | . | . | -2.23 | . | . |
| 20 | . | 2.27 | . | . | . | +2.04 | . | . | -3.16 | . | . |
| 10 | . | 3.48 | . | . | . | . | . | . | -3.22 | . | . |
| 0 | . | 3.63 | . | . | . | . | . | . | -3.27 | . | . |
| | | | | | | DATA SET II | | | | | |
| 40 | . | 2.03 | . | . | . | +6.17 | -4.69 | . | . | . | . |
| 30 | . | 3.71 | . | +1.50 | . | +5.97 | -8.05 | . | . | . | -1.12 |
| 20 | . | 6.16 | . | +3.92 | . | +3.36 | -10.70 | . | . | . | . |
| 10 | . | 8.03 | . | +5.03 | . | . | -10.50 | . | . | . | . |
| 0 | . | 8.21 | . | +5.38 | . | . | -10.40 | . | . | . | . |

Table 13. Examples of significant balances of ZKE for polar caps with various upper boundaries (Rosen method). Units are $10^{20}$ erg $sec^{-1}$.

| 1013 mb to | {1} | {3"} | {6's} | {10} | {12's} | vs {1} | {4} | {6's} | {7} | {10} | {12's} |
|---|---|---|---|---|---|---|---|---|---|---|---|
| **SYMMETRIC EQUATION** | | | | | | | | | | | |
| **DATA SET I** | | | | | | | | | | | |
| 913 | . | . | . | 3.24 | +1.05 | -1.37 | -1.24 | -1.02 | . | . | . |
| 613 | 5.04 | . | . | +6.01 | +1.67 | . | -8.29 | -4.46 | . | . | . |
| 313 | 12.20 | +1.72 | . | +10.10 | . | . | -16.20 | -2.88 | . | . | -5.03 |
| 113 | 21.60 | +3.66 | . | . | . | . | -17.50 | -2.73 | . | . | -2.39 |
| 13 | 18.60 | +3.63 | . | . | . | . | -17.80 | -3.27 | . | . | . |
| **DATA SET II** | | | | | | | | | | | |
| 913 | 1.99 | . | . | +1.78 | +2.63 | . | . | -.59 | -3.00 | . | . |
| 613 | 11.20 | +.97 | . | . | . | . | -4.12 | . | -.90 | -2.50 | -1.20 |
| 313 | 7.97 | +3.93 | +4.77 | +7.42 | . | . | -13.70 | . | . | . | -7.66 |
| 113 | 5.68 | +7.95 | +5.69 | +.90 | . | . | -14.70 | . | . | . | -1.82 |
| 13 | 3.96 | +8.21 | +5.38 | . | . | . | -14.40 | . | . | . | . |

| | {1'} | {3"} | {6's} | {12's} | {1'} | {6's} | {12's} |
|---|---|---|---|---|---|---|---|
| **TRADITIONAL EQUATION** | | | | | | | |
| **DATA SET I** | | | | | | | |
| 913 | . | . | . | 1.05 | . | -1.02 | . |
| 613 | 2.73 | . | . | +1.67 | . | -4.46 | . |
| 313 | 6.61 | +1.72 | . | . | . | -2.88 | -5.03 |
| 113 | 2.49 | +3.66 | . | . | . | -2.73 | -2.39 |
| 13 | . | 3.63 | . | . | . | -3.27 | . |
| **DATA SET II** | | | | | | | |
| 913 | . | . | . | 2.63 | . | -.59 | . |
| 613 | 3.44 | +.97 | . | . | . | . | -1.20 |
| 313 | 2.40 | +3.93 | +4.77 | . | . | . | -7.66 |
| 113 | . | 7.95 | +5.69 | . | -8.50 | . | -1.82 |
| 13 | . | 8.21 | +5.38 | . | -10.40 | . | . |

both data sets. The examples were chosen so as to more clearly show how individual terms change nature with polar cap size, data set and mathematical formulation.

As for the cause of residuals, several possible explanations have already been offered. Certainly the approximations inherent in the mathematical formulations are a source of error, particularly the assumptions at the ground and top of the atmosphere, the constancy of $\rho$ in the horizontal, and the neglect of possible storage effects. But, as pointed out by the tables just presented, data has to be considered a very possible cause of residuals. There may be systematic bias because of missing data, especially at upper levels where the residuals tend to misbehave as previously mentioned. Stoldt (1971) investigated this point for the N. Hemisphere data set, and found it to be negligible. But with the scarcity of the present S. Hemisphere data set, the effect could be quite significant. There may be bias because of the differences in coverage over land and water areas. Walker (1970) researched this effect for the N. Hemisphere, and also found it to be negligible for most terms. But again, with the much smaller S. Hemisphere data set and the greater fraction of ocean surface, this type of bias may certainly be something to be reckoned with.

However, the error in assuming the lower boundary

is always at 1013 mb may be the prime cause of residuals, particularly for polar caps bounded below the jet stream level. For example, one might have expected the addition of bogus stations to decrease residuals by reducing any land-ocean bias in the original data set. That this is not the case might be explained as follows. The bogus stations produce stronger surface winds as seen on Figure 2. If the mathematical formulation at the ground is incorrect to the extent that much of the destruction of ZKE by surface friction is missed because of the above assumption as previously suggested, then the demand of increased destruction because of increased surface winds, due to the addition of bogus stations, is also missed. Thus the residuals may be greater. It should be noted that since the S. Hemisphere has so much more ocean surface than the N. Hemisphere, the loss of ZKE by the atmosphere to drive the oceanic circulations is no doubt also much greater. This could also have significant consequences at the lower boundary.

Finally, there are sources of error in the machine techniques used for the calculations. Round off errors are probably too small to have an effect. But how much of an effect does the machine zonal averaging and horizontal analysis processes have? It is possible that these techniques, used so successfully in the N. Hemisphere studies,

may not work effectively with the much scarcer data set of the S. Hemisphere. It may smooth out too much of the actual fields, particularly since initial guess fields are not weighted very heavily, and the resulting fields may not be a true reflection of the actual data set.

# CHAPTER V

## CONCLUDING REMARKS

It is not my intention to compare in detail all of the present results to previous S. Hemisphere and N. Hemisphere studies. Due to the difficulty of obtaining sufficient quantities of reliable S. Hemisphere data, different studies of the S. Hemisphere general circulation seldom agree with each other in detail. Although the precise magnitudes and spatial distributions of the quantities investigated in the present study are not expected to exactly correspond to those of previous studies, one may get a feeling for the more important features of the S. Hemisphere circulation and the processes that act to maintain it. In any case, a few key comparisons of important quantities with those of previous works may provide at least a partial basis for deciding which of our sets is more reliable.

There are major differences between the two data sets when considering the wind statistics. Set II has more westerlies with a jet of 26.0 m $sec^{-1}$ at 44S, compared to 20.7 m $sec^{-1}$ at 43S for set I. The corresponding figure from Obasi, 1963, is 35.4 m $sec^{-1}$ at 30S for the period April - September, and a little less than 25.0 m $sec^{-1}$ centered in the 35 - 50S region for October - March. The winter season also shows another jet in the lower stratosphere at high latitudes. From a study by Heastie and

Stephenson, 1960, $[\bar{u}]$ is over 30 m sec$^{-1}$ at 45S in January, and has the same value around 30S in July. Obviously data set II agrees much more than set I with previous works.

The other vital statistic in the wind group is the mass stream function, $\psi$ . Which meridional circulation seems more reasonable? On the face of it, I would say set II gives a more realistic picture. It is difficult to accept the indirect cell above a direct cell circulation of set I in mid-latitudes on the basis of previous studies. From Starr, Peixoto and Gaut (1970), the N. Hemisphere meridional circulation consists of a classical three cell pattern. The low latitude Hadley Cell has a maximum strength of over $20 \times 10^{12}$ gm sec$^{-1}$, while the mid-latitude Ferrel Cell has a strength of over $-35 \times 10^{12}$ . This is similar to our results for set II, where the corresponding values are $23.7 \times 10^{12}$ and $-33.4 \times 10^{12}$ , although the Hadley Cell covers a smaller latitudinal extent and the Ferrel Cell a larger extent than those for the N. Hemisphere. The mode of calculation in Starr et. al. was the same as that in the present study.

Newell et. al. (1973) calculated a S. Hemisphere meridional circulation from direct observations of $[\bar{v}]$ to 20S, and indirectly from horizontal eddy transports of momentum from 20S to 90S. They arrive at a three cell pattern similar to that of the N, Hemisphere. Their values for the Hadley Cell center are on the order of $40 \times 10^{12}$ gm sec$^{-1}$

for December - February, and $200 \times 10^{12}$ for June - August. For the Ferrel Cell their values are $-30$ to $-35 \times 10^{12}$ for both seasons. Gilman (1965) also inferred the circulation from Obasi's values for the horizontal eddy transports of momentum and the mean zonal wind. His yearly values are about $70 \times 10^{12}$ gm sec$^{-1}$ for the Hadley Cell, and $-20 \times 10^{12}$ for the Ferrel Cell.

It is to be noted that the indirect method based on horizontal eddy transports of momentum neglects vertical eddy transports except in the surface layer where the stress is assumed to decrease linearly with pressure from a predetermined surface value. It is uncertain whether this method is more, or less, reliable than that of direct evaluation from $[\overline{vu}]$ with all the uncertainties inherent in the latter. However, the a priori neglect of possibly important vertical eddy transports of momentum acting in a negative viscous sense does not appeal to the present investigator.

A study of the horizontal transports of momentum calculated by Obasi also indicates data set II may be more realistic. Obasi's polewards maximum of transient eddy transport is roughly $-120 \times 10^{21}$ cm$^4$ sec$^{-2}$ for the yearly average compared to $-91.9 \times 10^{21}$ for set II and $-63.6 \times 10^{21}$ for set I. Also, in Obasi's work, the standing eddy transport is least important, but the horizontal mean cell

transport has a significant equatorwards maximum of about $42 \times 10^{21}$ cm$^4$ sec$^{-2}$ for the yearly average. For sets I and II, we find values of $13.7 \times 10^{21}$ and $43.6 \times 10^{21}$ respectively. The results from Obasi compare much more favorably with our previous discussion for the results of set II. Despite the differences in the horizontal momentum transports in sets I and II, it is significant that both sets have the transient eddy transports dominating over the standing eddy and mean cell transports, as was true for the N. Hemisphere study of Starr et. al., indicating that the process of negative viscosity in the horizontal is an important one in general circulation mechanics.

There have been no previous calculations for the vertical eddy transports of momentum in the S. Hemisphere. Gilman (1964) did attempt to calculate an empirical coefficient of eddy viscosity using Obasi's data on horizontal eddy momentum transports and mean zonal wind. However, he did not consider his numerical results to be significant. It is encouraging that both data sets show negatively viscous upward transports into the jet, and downward transports in the regions of maximum surface westerlies as was true for the N. Hemisphere study by Starr, Peixoto and Sims (1970). Also interesting is the fact that the cross sections for both data sets show a dip in the zero line around 40S below the jet stream. This feature was also evident on the N. Hemisphere cross section in the

40 - 50N range.

Likewise, the complete zonal kinetic energy equation has for the first time been evaluated for the S. Hemisphere, and the results for both sets are at least reasonable, although somewhat contradictory. This in itself is encouraging considering the limited data available. Listed below are the important terms in the hemispheric balance of ZKE for sets I and II and the corresponding N. Hemisphere balance from Rosen, 1970. Units are $10^{20}$ erg $sec^{-1}$.

| | Symmetric | | | Traditional | | |
|---|---|---|---|---|---|---|
| | $\{1\}+\{3''\}+\{6's\}$ | vs | $\{4\}+\{6's\}$ | $\{3''\}+\{6's\}$ | vs | $\{1'\}+\{6's\}$ |
| Set I | 18.60+3.63 | | -17.80-3.27 | 3.63 | | -3.27 |
| Set II | 3.96+8.21+5.38 | | -14.40 | 8.21+5.38 | | -10.40 |
| N.H. | 17.50+7.03 | | -23.60 -.97 | 7.03 | | -5.19 -.97 |

In the symmetric formulation, the same four processes dominate in each case, with some differences. In particular, the negative generation by vertical eddies of set I agrees more with the N. Hemisphere result than the large positive generation of set II. The large values of $\{1\}$ and $\{4\}$ of set I also agree well with the N. Hemisphere results. However the large value for the horizontal transient eddy term of set II agrees well with the N. Hemisphere values. In the traditional equation, the value of $\{1'\}$ for set II is twice as large as that of the N. Hemisphere, while set I indicates a negligible value for $\{1'\}$. In any case, the very fact that most of the same processes appear to

be important in both hemispheres is encouraging in itself. Since the values listed above often arise as differences between large numbers of oppositie signs, it is not surprising that the agreement is not better.

There is no way to state absolutely which of our sets of results is more accurate. Set I satisfies the mathematical criteria of small vertically averaged $[\tilde{\omega}]$ and small residuals better than set II. But set II appears to give results more compatible with previous works in most instances.

In the final analysis, the present study must be considered an experiment. The most extensive S. Hemisphere data set yet compiled has been used to calculate some statistics previously considered by other investigators, and some statistics for the first time. It is obvious that even this data set is insufficient to make any detailed definitive statements concerning the S. Hemisphere circulations. As proof of this, all one need do is to note the significant differences produced by the addition of a mere 26 bogus stations. One can not consider any of the results presented to completely and accurately reflect what is actually happening in the S. Hemisphere atmospheric circulation. Indeed, this must be said of any work concerning the S. Hemisphere, past or present. The limited data available to all investigators precludes any really reliable analysis. It is thus impossible to state the

present results are definitely better, or for that matter worse, than any other previous S. Hemisphere study.

Obviously, the era of a sufficient network of observing stations in the S. Hemisphere is years away due to the preponderance of underdeveloped nations and the prohibitive cost of weather ships. The question arises as to whether all that can be done in the meantime has been done. It is possible that the method of using bogus stations presented herein could be improved upon. Several alternatives are listed below.

1) An obvious thing to do would be to use a different network of bogus stations, presumably increasing the size of the network. The results would then no doubt be different, but probably not more reliable. It must be realized that the values used for $\bar{u}$, $\bar{v}$ and $\overline{u'v'}$ at any bogus station are not measured but inferred. No one has actual data in the large data scarce ocean areas, particularly the Pacific. The wind fields in these areas are inferred from analysis over adjoining areas with good coverage, intuition, and whatever slight observational evidence is available. It is felt that Obasi's analyses in these areas are as good as any previously published. Any additional bogus stations would still have only guessed data, and would not really improve the reliability of the present calculations.

2) An alternative in the same vein as the first would

be to hand analyze or machine analyze the wind fields only in those regions where the present data set has an acceptable station coverage. The remaining areas would then be hand analyzed, basing your guesswork upon analyses in the good coverage areas and using Obasi's work as guidance. Data for bogus stations could then be picked off these analyses, or the analyses themselves could be considered the final horizontal wind fields. As there are nine pressure levels to do this for, it is doubtful that the end result would warrant the time and expense spent in preparing it.

3) A completely different approach would involve the initial guess fields. As the machine techniques are set up now, the initial guess fields are not weighted very heavily. It is generally felt that Crutcher's data, which is used as the initial guess field at 1000 mb in the present study, is fairly reliable based on ship reports. It might be profitable to use Crutcher's 1000 mb data as actual data, and the original data set would provide the initial guess field. It is also suggested that the initial guess fields at the other levels, which are the final analyses at the level below, be weighted more heavily. This could conceivably improve the $\bar{u}$ and $\bar{v}$ analyses to a significant extent. The problem here is that the horizontal eddies play a very important role, and the above scheme can not be applied to them because of lack of

information at the surface.

4) The most profitable course of action would probably be some combination of 2) and 3). It is impossible to speculate how much this would improve the present results, but it would be an interesting experiment.

In conclusion, all I can really feel confident in stating is that a comprehensive attempt has been made to fill in some of the empty spots in our knowledge of the general circulation of the Southern Hemisphere, and at the very least the results presented give an indication of what processes may be important in maintaining that circulation. As for detailed and highly reliable information, this must come in the future when sufficient data becomes available.

ACKNOWLEDGMENTS

For Professor Victor P. Starr, who suggested the topic herein investigated and whose guidance in writing this thesis was invaluable, I express my sincere appreciation.

Special thanks are due Mr. R. Rosen whose suggestions and comments were most helpful, as well as Mr. L. Reed of Environmental Research Technology Corp. who performed the calculations, Miss I. Kole who drafted the figures, and my wife Marjorie who typed the manuscript.

Finally, I am grateful to the National Science Foundation for granting me a fellowship to support my graduate studies. Funds for this research were also provided by N.S.F. under grant no. GA-36021X.

BIBLIOGRAPHY

Frazier, H.M., E.R. Sweeton and J.G. Welsh, 1968: Data Processing Support to a Program for Observational and Theoretical Studies of Planetary Atmospheres, progress report, Traveler's Research Center, Hartford, Conn., 87 pp.

Gilman, P.A., 1964: On the Vertical Transport of Angular Momentum in the Atmosphere, Pure and Applied Geophysics, 57, 161-166.

Gilman, P.A., 1965: The Meridional Circulation of the Southern Hemisphere Inferred from Momentum and Mass Balance, Tellus, 17, 277-284.

Heastie, H., and P.M. Stephenson, 1960: Upper Winds over the World, Parts I and II, Geophys. Mem. no. 103, Meteor. Off. London, H.M. Stationary Off., 217 pp.

Jeffreys, H., 1926: On the Dynamics of Geostrophic Winds, Quarterly Journal of the Royal Meteor. Soc., 52, 85-104.

Lorenz, E.N., 1967: The Nature and Theory of the General Circulation of the Atmosphere, World Meteorological Organization, Geneva, 161 pp.

Newell, R.E., J.W. Kidson, D.G. Vincent and G.J. Boer, 1973: The General Circulation of the Tropical Atmosphere and Interactions with Extra-Tropical Latitudes, M.I.T. Press, in press.

Newton, C.W., 1971a: Mountain Torques in the Global Angular Momentum Balance, J. of Atmospheric Sciences, 28, 623-628.

_____, 1971b: Global Angular Momentum Balance: Earth Torques and Atmospheric Fluxes, J. of Atmospheric Sciences, 28, 1329-1341.

Obasi, G.O.P., 1963a: Atmospheric Momentum and Energy Calculations for the Southern Hemisphere During the IGY, Scientific Rep. #6, Planetary Circulations Proj.,M.I.T., 354 pp.

_____, 1963b: Poleward Flux of Atmospheric Angular Momentum in the Southern Hemisphere, J.A.S., 20, 516-528.

_____, 1965: On the Maintenance of the Kinetic Energy of Mean Zonal Flow in the Southern Hemisphere, Tellus, 17, 96-105.

Phillips, N.A., 1963: Geostrophic Motion, Review of Geophysics, 1, 123-176.

Rosen, R.D., 1970: Generation and Vertical Transport of Zonal Kinetic Energy, S.M. Thesis, M.I.T., 126 pp.

_____, 1971: Vertical Transport of Mean Zonal Kinetic Energy from Five Years of Hemispheric Data, Tellus, 24, 302-309.

_____, 1972: Effects of the Earth's Rotation and the Balance of Zonal Kinetic Energy, Pure and Applied Geophysics, 95, 192-220.

Sims, J.E., 1969: Evaluation of the Symmetrical Zonal Kinetic Energy Equation, S.M. Thesis, M.I.T., 84 pp.

_____, 1970: Meridional Transport of Mean Zonal Kinetic Energy from Five Years of Hemispheric Data, Tellus, 22, 655-662.

Starr, V.P., 1948: An Essay on the General Circulation of the Earth's Atmosphere, J. of Meteorology, 5, 39-43.

_____, 1948: On the Production of Kinetic Energy in the Atmosphere, J. of Meteorology, 5, 193-196.

_____, 1968: Physics of Negative Viscosity Phenomena, McGraw-Hill, New York, 254 pp.

_____ and N.E. Gaut, 1969: Symmetrical Formulation of the Zonal Kinetic Energy Equation, Tellus, 21, 185-192.

_____ and B. Saltzman, 1966: A Compilation of Observational Studies of the Atmospheric General Circulation, Scientific Report #2, Planetary Circulations Project, M.I.T., 700 pp.

_____ and J.E. Sims, 1970: Transport of Mean Zonal Kinetic Energy in the Atmosphere, Tellus, 22, 167-171.

_____ and R.M. White, 1951: A Hemispherical Study of the Atmospheric Angular Momentum Balance, Quarterly J. of the Roy. Meteor. Soc., 77, 215-225.

_____, J.P. Peixoto and N.E. Gaut, 1970: Momentum and Zonal Kinetic Energy Balance of the Atmosphere from Five Years of Hemispheric Data, Tellus, 22, 251-274.

Starr, V.P., J.P. Peixoto and J.E. Sims, 1970: A Method for the Study of the Zonal Kinetic Energy Balance in the Atmosphere, Pure and Applied Geophysics, 80, 346-358.

Stoldt, N.W., 1971: Effects of Missing Data on Zonal Kinetic Energy Calculations, Pure and Applied Geophysics, 92, 207-218.

Van Loon, H., J.J. Taljaard, R.L. Jenne and H.L. Crutcher, 1971: Climate of the Upper Air: Southern Hemisphere, NCAR Technical Notes, #NCAR-TN/STR-57.

Walker, H.C., 1970: Unbiased Station Grid for the Study of the Kinetic Energy Balance of the Atmosphere, Pure and Applied Geophysics, 81, 313-322.

White, R.M., 1949: The Role of Mountains in the Angular Momentum Balance of the Atmosphere, J. of Meteorology, 6, 353-355.